Experimental Neurology 236 (2012) 268–282

Contents lists available at SciVerse ScienceDirect

Experimental Neurology

journal homepage: www.elsevier.com/locate/yexnr

Regular Article

Inhibition of ROS-induced p38MAPK and ERK activation in microglia by acupuncture relieves neuropathic pain after spinal cord injury in rats

Doo C. Choi [a,b], Jee Y. Lee [a,b], Eun J. Lim [a,b], Hyung H. Baik [c], Tae H. Oh [a], Tae Y. Yune [a,b,c,*]

[a] Age-Related and Brain Diseases Research Center, School of Medicine, Kyung Hee University, Seoul 130-701, Republic of Korea
[b] Neurodegeneration Control Research Center, School of Medicine, Kyung Hee University, Seoul 130-701, Republic of Korea
[c] Department of Biochemistry and Molecular Biology, School of Medicine, Kyung Hee University, Seoul 130-701, Republic of Korea

ARTICLE INFO

Article history:
Received 17 December 2011
Revised 23 March 2012
Accepted 16 May 2012
Available online 23 May 2012

Keywords:
Acupuncture
Spinal cord injury
Central neuropathic pain
Microglia
MAPK kinase
Prostaglandin E2

ABSTRACT

Acupuncture (AP) is currently used worldwide to relieve pain. However, little is known about its mechanisms of action. We found that after spinal cord injury (SCI), AP inhibited the production of superoxide anion (O_2•), which acted as a modulator for microglial activation, and the analgesic effect of AP was attributed to its anti-microglial activating action. Direct injection of a ROS scavenger inhibited SCI-induced NP. After contusion injury which induces the below-level neuropathic pain (NP), Shuigou and Yanglingquan acupoints were applied. AP relieved mechanical allodynia and thermal hyperalgesia, while vehicle and simulated AP did not. AP also decreased the proportion of activated microglia, and inhibited both p38MAPK and ERK activation in microglia at the L4–5. Also, the level of prostaglandin E_2 (PGE2), which is produced via ERK signaling and mediates the below-level pain through PGE2 receptor, was reduced by AP. Injection of p38MAPK or ERK inhibitors attenuated NP and decreased PGE2 production. Furthermore, ROS produced after injury-induced p38MAPK and ERK activation in microglia, and mediated mechanical allodynia and thermal hyperalgesia, which were inhibited by AP or a ROS scavenger. AP also inhibited the expression of inflammatory mediators. Therefore, our results suggest that the analgesic effect of AP may be partly mediated by inhibiting ROS-induced microglial activation and inflammatory responses after SCI and provide the possibility that AP can be used effectively as a non-pharmacological intervention for SCI-induced chronic NP in patients.

Introduction

Neuropathic pain (NP) is one of the unfavorable pathological pains which are caused by damage or abnormal function of the peripheral or central nervous system (Baron, 2006). NP includes spontaneous burning pain or stimulus-evoked pain which is characterized by hyperalgesia (pain resulting from over response to a noxious stimulus) and allodynia (pain evoked by a non-noxious stimuli) (Woolf and Mannion, 1999). An average of 70–80% of the patients with spinal cord injury (SCI) usually experiences intractable central NP. SCI-induced NP can be localized above-, at-, and below-levels as rostral, same and caudal position from the injury site (Beric, 1997; Christensen and Hulsebosch, 1997; Siddall et al., 1997). Several studies for elucidation of the mechanisms underlying pain processing show that inflammatory responses are implicated in the SCI-induced NP at the below level (Christensen et al., 1996; Detloff et al., 2008; Peng et al., 2006). Furthermore, microglia are known to be involved in the development of SCI-induced NP at the below level (Detloff et al., 2008; Hains and Waxman, 2006; Hulsebosch, 2008; Tan et al., 2009).

Microglia activated after SCI release many inflammatory mediators including TNF-α, IL-1β, IL-6, COX-2, iNOS, and prostaglandin E2 (PGE2), which induces NP by sensitizing pain transmission neurons (Detloff et al., 2008; Hulsebosch, 2008; Peng et al., 2006; Zhao et al., 2007). As signaling molecules involved in NP processing after SCI, both p38MAPK and ERK are activated in microglia at L4–L5 level of spinal cord (Hains and Waxman, 2006; Zhao et al., 2007). The inhibition of microglial activation by minocycline, an anti-inflammatory drug, reduces SCI-induced below-level pain by attenuating p38MAPK and ERK activation in microglia after injury (Hains and Waxman, 2006; Tan et al., 2009; Zhao et al., 2007). Furthermore, PGE2 produced via ERK-dependent signaling in activated microglia mediates SCI-induced NP through EP2, PGE2 receptor, expressed in spinal neurons (Zhao et al., 2007).

Abbreviations: AP, Acupuncture; BBB, Basso–Beattie–Bresnahan; CNS, central nervous system; CNP, central neuropathic pain; COX-2, cyclooxygenase-2; DMSO, dimethyl sulfoxide; ERK, extracellular signal-regulated kinase; GM, gray matter; iNOS, inducible nitric oxide synthase; IL-1β, interleukin-1β; IL-6, interleukin-6; NP, neuropathic pain; p38MAPK, p38 mitogen-activated protein kinase; PWL, paw withdrawal latency; PWT, paw withdrawal threshold; POD, postoperative days; PGE2, prostaglandin E2; ROS, reactive oxygen species; RT, room temperature; SCI, spinal cord injury; TNF-α, tumor necrosis factor.

* Corresponding author at: Department of Biochemistry and Molecular Biology, School of Medicine, Kyung Hee University, Medical Building 10th Floor, 1 Hoegi-dong, Dongdaemun-gu, Seoul 130-701, Republic of Korea. Fax: +82 2 969 6343.
E-mail address: tyune@khu.ac.kr (T.Y. Yune).

0014-4886/$ – see front matter © 2012 Published by Elsevier Inc.
doi:10.1016/j.expneurol.2012.05.014

Several medications such as anti-convulsants, anti-depressants, channel blockers, and opioids are used to alleviate SCI-induced NP (Baastrup and Finnerup, 2008; Levendoglu et al., 2004; Parisod et al., 2003; To et al., 2002; Wang et al., 2005). However, SCI-induced NP can't be adequately alleviated by currently available medications. Acupuncture (AP) is known to relieve peripheral NP as well as acute or chronic inflammatory pain via inhibition of microglial activation followed production of inflammatory mediators in various pain models (Bernateck et al., 2008; Kang et al., 2007; Lau et al., 2008). Although the analgesic effect of AP has been well documented, the precise mechanism of AP's action on NP is still unknown.

Here we examined the analgesic effect of AP on SCI-induced NP after SCI. Our data show that AP effectively alleviated SCI-induced NP in part by inhibiting superoxide anion (O_2•) production and thereby reducing O_2•-induced p38MAPK and ERK activation in microglia and suppressing production of ERK-dependent PGE2 as well as inflammatory mediators after injury.

Materials and methods

Spinal cord injury

Adult rats [Sprague Dawley, male, 250–300 g; Sam:TacN (SD) BR; Samtako, Osan, Korea] were anesthetized with chloral hydrate (500 mg/kg) and a laminectomy was performed at the T9–T10 level, exposing the cord beneath without disrupting the dura. The spinous processes of T8 and T11 were then clamped to stabilize the spine, and the exposed dorsal surface of the cord was subjected to moderate contusion injury (10 g × 25 mm) using a New York University (NYU) impactor as described previously (Yune et al., 2007). For the sham-operated controls, the animals underwent a T9–T10 laminectomy without weight-drop injury. All surgical interventions and postoperative animal care were performed in accordance with the Guidelines and Polices for Rodent Survival Surgery provided by the Animal Care Committee of the Kyung Hee University.

Acupuncture

Acupuncture (AP) was applied at both GV26 and GB34 without anesthesia using an immobilization apparatus designed by our lab as described previously (Choi et al., 2010). In our previous report, we found that AP applied at GV26 and GB34 acupoints simultaneously was most neuroprotective by inhibiting microglial activation (Choi et al., 2010). Therefore, we anticipated that simultaneous AP treatment at GV26 and GB34 may also exert most analgesic effects after SCI. GB34 is located at the point of intersection of lines from the anterior border to the head of the fibula, and GV26, located at the mid points between base of the columnar nasi and the upper lip, on the facial midline (Yin et al., 2008) (Fig. 1A). Stainless-steel AP needles of 0.20 mm in diameter were inserted to a depth of 4–6 mm at each acupoint bilaterally, turned at a rate of two spins per second for 30 s, and then the needles were retained for 30 min. AP treatment was applied once a day on 31 to 33 d and pain behavioral tests were performed at 1 h after AP treatment. To confirm the effect of AP, we used rat received injury but not received any AP treatment and treated with simulated AP with a toothpick at each acupoint as described by Cherkin et al. (2009) and Choi et al. (2010) as controls.

Hindlimb locomotion

Examination of functional deficits after injury was conducted as previously described (Yune et al., 2007). To test hindlimb motor function, open-field locomotion was evaluated by using the Basso–Beattie–Bresnahan (BBB) locomotion scale as described (Basso et al., 1995). BBB is a 22-point scale (scores 0–21) that systematically and logically follows recovery of hindlimb function from a score of 0, indicative of no observed hind limb movements, to a score of 21, representative of a normal ambulating rodent.

Behavioral pain tests

All pain behavioral testing was performed by trained investigators who were blind as to the experimental conditions and began at post-operative days (POD) 28 to confirm behavioral signs of SCI-induced chronic NP before AP or drug treatment. For all experiments, we used only animals that chronic NP following SCI was developed. At POD 28, hindlimb locomotion of injured animals was recovered well enough to yield reliable withdrawal reflex as described previously (Hains et al., 2001).

Mechanical allodynia was assessed by the paw withdrawal threshold (PWT) in response to probing with a series of calibrated von Frey filaments (3.92, 5.88, 9.80, 19.60, 39.20, 58.80, 78.40 and 147.00 mN, Stoelting, Wood Dale, IL; equivalent in grams to 0.4, 0.6, 1.0, 2.0, 4.0, 6.0, 8.0 and 15.0). The 50% withdrawal threshold was determined by using the up-down method (Chaplan et al., 1994). In brief, rats were placed under transparent plastic boxes (28 × 10 × 10 cm) on a metal mesh floor (3 × 3 mm mesh). They were then left alone for at least 20 min of acclimation before sensory testing began. Testing was initiated with the filament which bending force was 19.60 mN, in the middle of the series. Von Frey filament applied to the plantar surface of each hindpaw, and the most sensitive spot of the hindpaw was first determined by probing various areas with the 19.60 mN filament. In the absence of a hindpaw withdrawal response to this filament, this process searching the sensitive spot was repeated with the next stiffer filament. However, if the sensitive spot by which a positive response had been elicited was determined, this spot was touched just one time with one of a series of 8 von Frey filaments in a up-down fashion, like following; a withdrawal response was cause to present the next weaker stimulus, and lack of withdrawal led to presentation of the next stronger stimulus. Stimuli were applied for 3–4 s to each hindpaw while the filament was bent and were presented at intervals of several seconds. A brisk hindpaw withdrawal to von Frey filament application was regarded as a positive response.

Heat sensitivity was assessed according to the Hargreaves method (Hargreaves et al., 1988) to determine paw withdrawal latency (PWL) in response to a radiant heat (Model 390, IITC Life Science Inc. Woodland Hills, CA). Animals were habituated to the apparatus, which consisted of six individual Perspex boxes on an elevated glass table. A radiant heat source under the glass table was focused on center of the plantar surface. The heat intensity was set to produce PWL of approximately 10 s in normal animals, and the cut-off time was set at 20 s to prevent tissue damage as reported (Liu et al., 2007; Zhang et al., 2007). Three times of heat stimuli were given for each paw at an interval of 5–10 min. The mean of PWL for three trials was taken for each paw of each rat.

Drug administration

Minocycline (Sigma, St. Louis, MO) was dissolved in normal saline and administrated i.p. (22.5 mg/kg) twice daily for 3 d by starting from POD 31 as previously described (Yune et al., 2007). Both p38MAPK inhibitor, SB203580 and ERK inhibitor, PD98059 (Merk Calbiochem, Darmstadt, Germany) were dissolved in 2% dimethyl sulfoxide (DMSO) and ROS scavenger, Mn (III) tetrakis (4-benzoic acid) porphyrin (MnTBAP, Merk Calbiochem) was dissolved in normal saline. SB203580 (10 μg/rat), PD98059 (10 μg/rat) and MnTBAP (2.5 mg/kg) were administered intrathecally with 5 or 10 μl once on POD 31.

For intrathecal injection, we used direct lumbar puncture according to the previously reported methods (Hylden and Wilcox, 1980; Mestre et al., 1994). In brief, experimental animals were anesthetized with 4% isoflurane in a mixture of O_2 gas. The lumbar

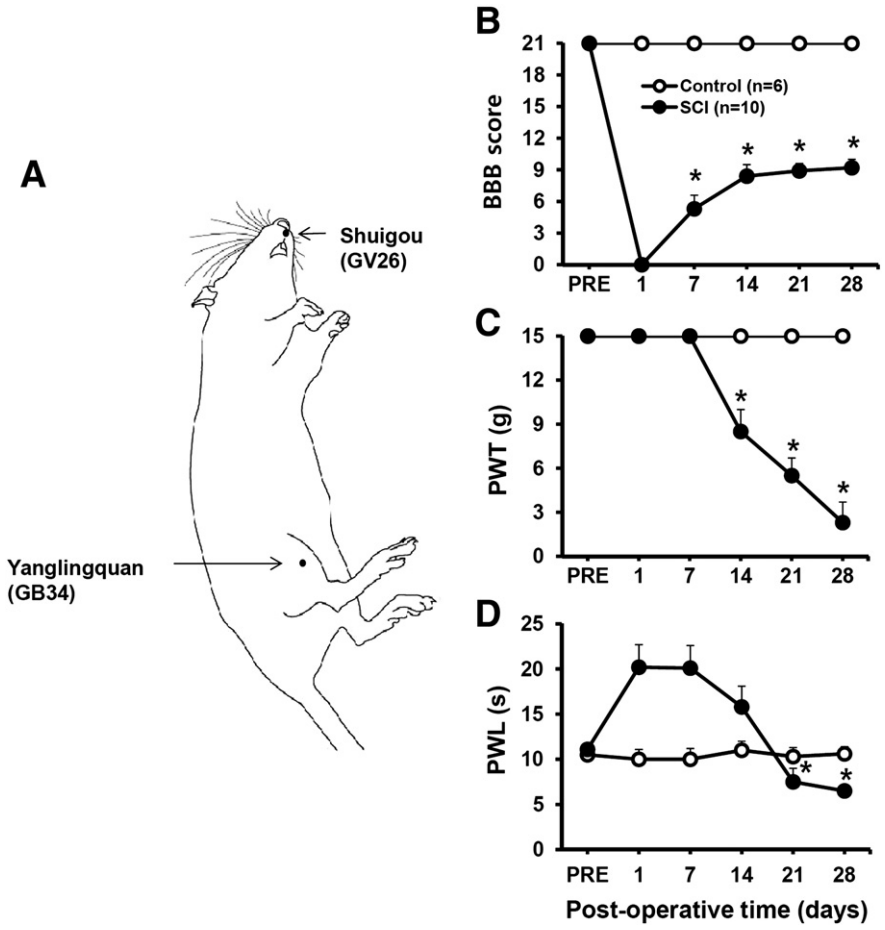

Fig. 1. Neuropathic pain at below level develops after SCI. (A) Schematic diagram showing acupoints applied to SCI animals. Acupuncture was applied at two specific acupoints, Shuigou (GV26) and Yanglingquan (GB34), throughout experiments. (B) Motor function as assessed by BBB scores after SCI. $^{*}p<0.05$. (C and D) Pain responses to mechanical stimuli (PWT) and heat stimuli (PWL) after injury (n = 6 for control; n = 10 for SCI). $^{*}p<0.05$.

vertebrae just cranial to both iliac crests were held by the thumb and middle finger, and the sixth lumbar (L6) spinous process was identified as located by palpating the highest spinous process with the index finger. A 26-gauge needle connected to a 25 μl Hamilton syringe was inserted from the caudal end, immediately lateral to the L6 spinous process at a 45° angle to the vertebral column and was pushed slowly in the cranioventral direction. The needle is inserted into the tissue to one side of the L5 or L6 spinous process so that it slips into the groove between the spinous and transverse processes. The needle is then moved carefully forward to the intervertebral space as the angle of the syringe is decreased to about 10°. The tip of the needle is inserted so that approx. 0.5 cm is within the vertebral column. Identification of the needle in the intrathecal space was based on the presence of a sudden lateral tail movement that occurred after penetration of the ligamentum flavum. Once the needle was in the intrathecal space, a dose of drug was injected slowly for 10 s. As a vehicle control, normal saline or normal saline containing 2% DMSO was injected during the same time points in separate injured animals.

Tissue preparation

At POD 31 or 33, 1 h after the last treatment with AP, minocycline, simulated AP, MnTBAP and vehicle, rats were anesthetized with chloral hydrate (500 mg/kg) and perfused via cardiac puncture initially with 0.1 M phosphate buffered saline (PBS, pH 7.4) and subsequently with 4% paraformaldehyde in PBS. L4–L5 segments of spinal cord were dissected out, post-fixed by immersion in the same fixative for 2 h and placed in 30% sucrose in PBS. The segment was embedded in OCT for frozen sections as previously described (Yune et al., 2007), and cross sections were then cut at 16 μm on a cryostat (CM1850; Leica, Wetzlar, Germany).

In situ detection of superoxide anion

The production of superoxide anion (O_2•) after SCI was examined by the in situ detection of oxidized hydroethidine (HEt) using HEt dye (Invitrogen, Carlsbad, CA). HEt is oxidized to the fluorescent ethidium (Etd) by O_2• (Bindokas et al., 1996) and is considered as an indicator of intracellular O_2•. At POD 31, HEt (stock solution 100 mg/ml) in DMSO was diluted to 1 mg/ml in PBS just before use, and 200 μl of HEt was injected intravenously at 15 min before AP or MnTBAP treatment as described (Yune et al., 2008). One hour after AP treatment, animals were cardinally perfused and spinal cord sections were prepared as described above. The fluorescence was assessed microscopically at Ex = 510–550 nm and Em > 580 nm for Etd detection and photographed with an Olympus microscope (BX51, Olympus, Japan) with software accompanying the Cool SNAP camera (Roper Scientific Sarasota, FL). For quantitative analysis of Etd fluorescence, the area of tissue fluorescence in three coronal sections in each animal was

analyzed using Image MetaMorph software (Molecular devices, Sunnyvale, CA) as described (Yune et al., 2008).

Immunohistochemistry

Tissue sections were incubated in 3% hydrogen peroxide in PBS for 10 min at room temperature (RT) to inhibit endogenous peroxidase activity. After washing with Tris-buffered saline including 0.1% Triton X-100 (TBST), the sections were immersed in 5% normal serum (Vector Laboratories INC, Burlingame, CA) in TBST for 1 h at RT to block nonspecific binding. They were then incubated with a mouse anti-CD11b (OX-42; 1:200; Millipore, Billerica, MA) or a rabbit anti-EP2 (1:1000; Millipore) overnight at 4 °C, followed by biotinylated secondary Abs (Dako, Carpinteria, CA). The ABC method was used to detect labeled cells using a Vectastain kit (Vector Laboratories INC). DAB served as the substrate for peroxidase. Some sections were processed for immunofluorescence and double labeling with Abs against phosphorylated-p38MAPK (p-p38MAPK, 1:100; Cell Signaling Technology, Danvers, MA), phosphorylated-ERK (p-ERK, 1:100; Cell Signaling Technology) and PGE2 receptor (EP2, 1:1000; Millipore). In brief, the sections were blocked in 5% normal serum in TBST for 1 h at RT and then incubated with primary Abs overnight at 4°C. Some sections stained for p-p38MAPK, p-ERK and EP2 were double-labeled using cell-type specific Abs for neurons (NeuN; 1:100; Millipore), microglia (OX-42; 1:200; Millipore), and astrocytes (GFAP; 1:10,000; Millipore). For double labeling, FITC or Cy3-conjugated secondary Abs (Jackson Immuno Research, West Grove, PA) were used. Nuclei were also labeled with DAPI according to the protocol of the manufacturer (Molecular Probes, Eugene, OR). In all controls, reaction to the substrate was absent if the primary Ab was omitted or replaced by a non-immune, control Ab. The immunofluorescent sections were mounted with Vectashield mounting medium (Vector). Fluorescence signal was detected by a fluorescence microscope (Olympus), and capture of images and measurement of signal co-localization was performed with MetaMorph.

Western blot

At POD 31 or 33, 1 h after the last treatment with AP, minocycline, simulated AP, MnTBAP and vehicle, whole lysates from L4–L5 segments of spinal cord were prepared with a lysis buffer containing 1% NP-40, 20 mM Tris, pH 8.0, 137 mM NaCl, 0.5 mM EDTA, 10% glycerol, 10 mM $Na_2P_2O_7$, 10 mM NaF, 1 μg/ml aprotinin, 10 μg/ml leupeptin, 1 mM sodium vanadate, and 1 mM PMSF. Tissue homogenates were incubated for 20 min at 4 °C, and centrifuged at 25,000 × *g* for 30 min at 4 °C. The protein concentration was determined using the BCA assay kit (Pierce, Rockford, IL). Protein sample (40 μg) was separated on SDS-PAGE and transferred to nitrocellulose membrane (Millipore). The membranes were blocked in 5% nonfat skim milk or 5% bovine serum albumin in TBST for 1 h at room temperature followed by incubation with Abs against p38MAPK (1:1000; Cell Signaling Technology), p-p38MAPK (1:1000; Cell Signaling Technology), ERK (1:1000; Cell Signaling Technology), p-ERK (1:1000; Cell Signaling Technology), iNOS (1:3000, Transduction Laboratory, Lexington, KY), COX-2 (1:1000, Cayman Chemical, MI) and β-Tubulin (1:10,000; Sigma) at 4 °C overnight. After washing, the membranes were incubated with HRP conjugated secondary Abs (Jackson Immuno Research) for 1 h and immunoreactive bands were visualized by chemiluminesence using Supersignal (Pierce). β-tubulin was used as an internal control. Relative intensity of each band to sham on Western blots was measured and analyzed by AlphaImager software (Alpha Innotech Corporation, San Leandro, CA). For doublets on western blot, e.g. ERK, we measured total intensity of the two bands. Background in films was subtracted from the optical density measurements. Experiments were repeated three times, and the values obtained for the relative intensity were subjected to statistical analysis. The blots shown in figures are representative of results from three separate experiments.

RNA isolation and RT-PCR

One hour after the last treatments at POD 33, RNA was isolated using TRIZOL® Reagent (Invitrogen) and 0.5 μg of total RNA was reverse-transcribed into first strand cDNA using MMLV according to the manufacturer's instructions (Invitrogen). For PCR amplifications, the following reagents were added to 1 μl of first strand cDNA: 0.5 U taq polymerase (Takara, Kyoto, Japan), 20 mM Tris–HCl, pH 7.9, 100 mM KCl, 1.5 mM $MgCl_2$, 250 μM dNTP, and 10 pmol of each specific primer. PCR conditions were as follows: denaturation at 94 °C, 30 s, primer annealing at indicated temperature, 30 s, and amplification at 72 °C, 30 s. PCR was terminated by incubation at 72 °C for 7 min. The primers used for TNF-α, IL-1β, IL-6, COX-2, iNOS and GAPDH were synthesized by the Genotech (Daejeon, Korea) and the sequences of the primers are as follows (5′–3′): IL-1β forward, 5′-GCA GCT ACC TAT GTC TTG CCC GTG-3′, IL-1β reverse, 5′-GTC GTT GCT TGT CTC TCC TTG TA-3′; (289 bp, 50 °C for 30 cycles); IL-6 forward, 5′-AAG TTT CTC TCC GCA AGA TAC TTC CAG CCA-3′; IL-6 reverse, 5′-AGG CAA ATT TCC TGG TTA TAT CCA GTT-3′ (240 bp, 58 °C for 30 cycles); TNF-α forward, 5′-CCC AGA CCC TCA CAC TCA GAT-3′; TNF-α reverse, 5′-TTG TCC CTT GAA GAG AAC CTG-3′ (215 bp, 56 °C for 28 cycles); COX-2 forward, 5′-CCA TGT CAA AAC CGT GGT GAA TG-3′; COX-2 reverse, 5′-ATG GGA GTT GGG CAG TCA TCA G-3′ (374 bp, 55 °C for 28 cycles); iNOS forward, 5′-CTC CAT GAC TCT CAG CAC AGA G-3′; iNOS reverse, 5′-GCA CCG AAG ATA TCC TCA TGA T-3′ (401 bp, 56 °C for 25 cycles); GAPDH forward, 5′-TCC CTC AAG ATT GTC AGC AA-3′; GAPDH, reverse, 5′-AGA TCC ACA ACG GAT ACA TT-3′ (308 bp, 50 °C for 23 cycles). The plateau phase of the PCR reaction was not reached under these PCR conditions. After amplification, PCR products were subjected to a 1.5% agarose gel electrophoresis and visualized by ethidium bromide staining. The relative density of bands (relative to sham value) was analyzed by the Alpha-Imager software (Alpha Innotech Corporation). Experiments were repeated three times and the values obtained for the relative intensity were subjected to statistical analysis. The gels shown in figures are representative of results from three separate experiments.

ELISA for PGE2 and cytokines

On POD 31 or 33, 1 h after the last treatments, levels of PGE2 and cytokines (TNF-α, IL-1β, and IL-6) in the lumbar spinal cords were assayed using prostaglandin E2 ELISA kit (Monoclonal; Cayman Chemical, Ann Arbor, MI) and cytokine ELISA kits (BioSource Europe, Nivelles, Belgium). Samples are as follows: sham (n = 4), veh (n = 4), minocycline (n = 4), PD98059 (n = 4), AP (n = 4), and PD98059 + AP (n = 4) for PGE2 at POD 31 and sham (n = 4), veh (n = 4), minocycline (n = 4), AP (n = 4), and simulated AP (n = 4) for cytokines at POD 33. Animals were deeply anesthetized with chloral hydrate (500 mg/kg, i.p.) and cardinally perfused. The lumbar spinal cord (L4–L5) was immediately removed after perfusion, weighed, and frozen in liquid nitrogen for storage at −80 °C. For analysis of PGE2, tissue was homogenized in ice-cold lysis buffer containing 1 mM EDTA, 10 μM indomethacin® (Cayman Chemical) in PBS using a tube pestle. Acetone was added (2× sample volume), and samples were centrifuged at 1500 × *g* for 10 min. The supernatants were then stored at −80 °C. The PGE2 monoclonal ELISA kit demonstrates sensitivity from 10 to 5000 pg/ml. Absorbance (412 nm) values of standards and samples were corrected by subtraction of the background value to correct for absorbance caused by nonspecific binding. For analysis of cytokines, tissues were homogenized and the levels of TNF-α, IL-1β, and IL-6 were assayed by ELISA and determined according to the manufacturer's instructions. All samples were analyzed in triplicate.

Quantitation of resting and activated microglia

To quantify resting and activated microglia in the L4–L5 spinal cord, coronal spinal cord sections (10 μm thickness) were collected (5 sections/animal) and labeled with OX-42 Ab. For quantitative analysis, OX-42 labeled sections were digitized and manually counted within preselected fields (100×100 μm) at lamina I–II (4 fields/animal). Resting and activated microglia were classified and counted based on a previous report (Hains and Waxman, 2006). Briefly, resting microglia displayed small compact somata bearing long, thin, and ramified processes, whereas activated microglia exhibited marked cellular hypertrophy and retraction of processes such that the process length was less than the diameter of the soma compartment. Cells were sampled only if the nucleus was visible within the plane of section and if cell profiles exhibited distinctly delineated borders (Hains and Waxman, 2006).

Statistical analysis

Data are presented as mean ± SD values. Comparison in between experimental groups was evaluated for statistical significance using either the paired Student's *t* test or the unpaired Student's *t* test. Multiple comparisons between groups were performed one-way ANOVA. Behavioral scores repeated for 3 d were analyzed by repeated measures ANOVA. Dunnett's case-comparison was used as Post hoc analysis. In all analyses, a p value of <0.05 was considered statistically significant. All statistical analyses were performed by using SPSS 15.0 (SPSS Science, Chicago, IL).

Results

Acupuncture relieves neuropathic pain developed after SCI

Acupuncture (AP) has long been employed as a treatment for numerous diseases including pain in Oriental medicine. We first examined whether chronic neuropathic pain (NP) is developed after SCI. Normal, un-operated rats showed normal levels of locomotor function (control group: BBB score; 21.0 ± 0.0), responses to mechanical (PWT; 15.0 ± 0.0 g) and thermal stimuli (PWL; 10.5 ± 0.6 s) (Figs. 1B, C, D). The hindlimbs were paralyzed immediately after injury, and the rats recovered extensive movement of hindlimbs within postoperative days (POD) 14 (Fig. 1B). On responses to innoxious, mechanical stimuli, injured rats were not responsive in cut-off level to mechanical stimuli up to POD 7, and thereafter, mechanical PWT decreased progressively (Fig. 1C). On responses to noxious and thermal stimuli, injured rats showed longer latency on POD 1 to POD 14 than normal control group and thereafter, decreased gradually (Fig. 1D). Since the motor function is damaged until POD 14 d, the higher values of PWL may be due to the loss of motor function. Then, NP from POD 14 for mechanical pain and POD 21 for thermal pain began to develop (Figs. 1C, D). At POD 28, for example, injured rats displayed mechanical allodynia and thermal hyperalgesia; the PWT and PWL of the hind paw to stimuli significantly decreased when compared with un-operated, normal control (SCI group: PWT; 2.5 ± 0.4 g; PWL; 6.0 ± 0.0 s, n = 10, vs. normal control group: PWT; 15.0 ± 0.0 g; PWL; 10.6 ± 0.8 s, n = 6, $p<0.05$) (Figs. 1C, D). Both PWT and PWL in sham-operated controls (n = 10) were not significantly different from normal control.

Next, we investigated the analgesic effects of AP on SCI-induced NP. In this study, we treated AP on two specific acupoints, Shuigou (GV26) and Yanglingquan (GB34) simultaneously throughout our experiments (Fig. 1A). Before AP treatment, all preselected spinal cord injured rats at POD 29 exhibited painful behaviors as showing the decrease of both mechanical PWT (SCI group: 2.7 ± 0.7 g) and thermal PWL (SCI group: 5.8 ± 0.3 s) (Figs. 2B, C) as compared to normal control group (see Figs. 1C, D). The injured rats were then divided randomly in each experimental group including vehicle, minocycline (positive control) (Hains and Waxman, 2006), AP and simulated AP (negative control) treatments and were treated for 3 d beginning from POD 31. Following treatment, there were no significant differences in BBB scores in all groups (BBB scores; 9–10, Fig. 2A). Vehicle treatment exhibited no significant effects on pain thresholds throughout testing period (Figs. 2B, C). However, AP treatment significantly increased mechanical PWT (AP group: 11.0 ± 1.6 g vs. vehicle group: 2.3 ± 0.8 g, n = 6, $p<0.001$), and thermal PWL (AP group: 9.1 ± 0.6 s vs. vehicle group: 5.9 ± 0.6 s, n = 6, $p<0.001$) when compared with vehicle group at POD 33 (Figs. 2B, C). Furthermore, the analgesic effect by AP was peaked at 1 h and continued for 3 h in mechanical allodynia and 2 h in thermal hyperalgesia (Figs. 5 and 7). Minocycline as a positive control also resulted in significant increases in PWT (minocycline group: 6.6 ± 1.6 g, n = 6, $p<0.001$) and PWL (minocycline group: 8.0 ± 0.4 s, n = 6, $p<0.001$) at POD 33 (Figs. 2B, C) and the analgesic effect was also continued for 2 h in both mechanical allodynia and thermal hyperalgesia (data not shown). By contrast, simulated AP treatment showed no significant effects on PWT (simulated AP group: 1.9 ± 0.7 g, n = 6) and PWL (simulated AP group: 5.5 ± 0.6 s, n = 6) as compared to vehicle group (Figs. 2B, C). Cessation of AP or minocycline treatment resulted in loss of their antinociceptive effect (Figs. 2B, C). These results indicate that AP has significant analgesic effects on SCI-induced mechanical allodynia and thermal hyperalgesia. Stress initiates a cascade of neuronal and hormonal responses aimed at protecting the organism and restoring homeostasis. It has also been reported that under stressful conditions, pain perception and reaction can be suppressed in favor of adaptive behaviors (Amit and Galina, 1986; Ford and Finn, 2008). Since restrain condition was applied during AP in our study, we determined whether the restrain might induce stress-related analgesic effects. As shown in Figs. 2D and E, both PWT and PWL were not significantly different between restrain and non-restrain animals. These data indicate that restrain condition used in the present study did not influence on the analgesic effects by AP.

Acupuncture inhibits microglial activation after SCI

Under normal condition, the resting microglia display a small soma bearing thin-branched processes. When activated by stimuli such as trauma, ischemia or inflammation, microglial soma becomes hypertrophic and exhibits the long and thin processes withdraw to resemble an amoeboid-like structure. These morphological changes are characteristics of the so-called activated microglia. Furthermore, activated microglia have been implicated in the development of NP after SCI (Hains and Waxman, 2006). To examine the effects of AP on microglial activation in the L4–L5 spinal cords, immunohistochemistry using an Ab against OX-42 was performed on POD 33 after 3 d treatments. Microglia were counted in the superficial layer (laminae I–II layers) of spinal dorsal horn where the majority of unmyelinated Aδ and C fibers involving in nociceptive signal processing and large-myelinated Aβ fibers are terminated (Fig. 3A). The number of resting or activated microglia was quantified by counting OX-42-positive cells with processes longer/shorter than the soma diameter (Figs. 3B, C). In sham control, the morphology of OX-42-positive cells displayed a small soma bearing thin-branched or ramified processes indicating a resting state (Fig. 3B, Sham). After injury, OX-42-positive cells displayed as a significant activated morphology demonstrating marked cell bodies hypertrophy and retraction of cytoplasmic processes (Fig. 3B, Veh). Quantitative analysis revealed a higher proportion of activated microglia (70.0 ± 0.52%) in vehicle group than in sham control (5.7 ± 0.32%) (Fig. 3C). After SCI, AP treatment significantly reduced the proportion of microglia with activated morphology when compared with vehicle control group (AP group: 37.1 ± 0.62% vs. vehicle group: 70.0 ± 0.52%; n = 5, $p<0.01$) (Figs. 3B, C). Minocycline treatment also resulted in a significant reduction in the proportion of activated microglia as compared to vehicle control (minocycline group: 35.0 ± 0.62%, n = 5, $p<0.01$) (Figs. 3B, C) as reported previously (Hains and Waxman, 2006). To confirm the

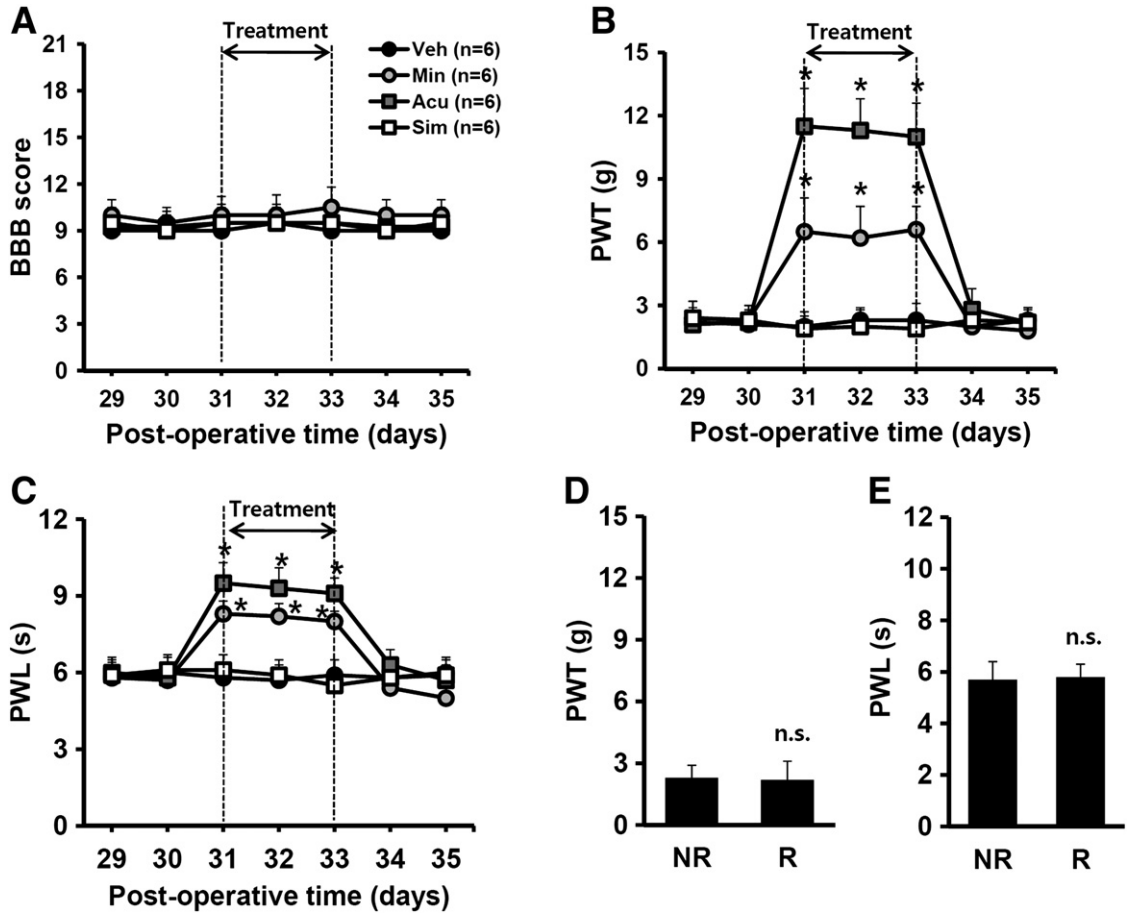

Fig. 2. Acupuncture relieves neuropathic pain after SCI. Rats with SCI-induced NP were treated with AP from POD 31 to POD 33 and analgesic effects of AP were examined (n = 6). (A) There was no significant difference in BBB scores in all groups throughout testing period. (B and C) AP or minocycline treatment significantly increased PWT (B) and PWL (C) when compared with those in the vehicle control after injury. Note that simulated AP had no significant effect on pain behavior. *$p<0.001$. Pain responses to mechanical stimuli (D) and heat stimuli (E) were not significantly different between non-restrain (NR) and restrain (R) animals (n = 10/group) at 31 d after injury. n.s. not significant.

specificity of AP effect on NP, simulated AP was applied to injured rats with a toothpick as described (Cherkin et al., 2009; Choi et al., 2010). Morphology of OX-42-positive cells in simulated AP group exhibited similar to that in vehicle control (Fig. 3B), and the proportion of activated microglia was not changed as compared to vehicle control (simulated AP group: 66.3 ± 1.42%, n = 5) (Fig. 3C). OX-42-positive cells were also not observed in the negative control in the absent of primary Ab (Fig. 3B, Control). These results indicate that microglia were activated in L4–L5 spinal dorsal horn at delayed time, and AP treatment significantly attenuated microglial activation after SCI.

Acupuncture inhibits p38MAPK activation after SCI

Since p38MAPK is activated in microglia and implicated in CNP following SCI (Crown et al., 2006; Hains and Waxman, 2006), we examined whether AP inhibits p38MAPK activation in microglia, thereby alleviating SCI-induced NP. First, using total protein extracted from L4–L5 spinal cords of rats treated with vehicle, minocycline, AP and simulated AP for 3 d from POD 31, we examined the protein level of p-p38MAPK by Western blot analysis. After SCI, the level of p-p38MAPK was increased as compared to sham control (data not shown) as reported (Hains and Waxman, 2006) and minocycline treatment significantly decreased the level of p-p38MAPK (minocycline group: 0.5 ± 0.06 vs. vehicle group: 1.0 ± 0.0; n = 4, $p<0.05$) (Fig. 4A). Furthermore, AP also decreased the level of p-p38MAPK, whereas simulated AP did not. Quantitative analysis shows that AP significantly decreased the level of p-p38MAPK when compared with vehicle or simulated AP-treated groups (AP group: 0.47 ± 0.06 vs. vehicle group: 1.0 ± 0.0 or vs. simulated AP group: 0.95 ± 0.04; n = 4, $p<0.05$) (Fig. 4B).

To examine whether p38MAPK is activated in the L4 dorsal horn of the spinal cord, immunohistochemical analysis using an Ab against p-p38MAPK was carried out. In sham-operated rats, p-p38MAPK-positive cells were not detected (Fig. 4C, Sham) as reported (Hains and Waxman, 2006). However, at POD 33, numerous p-p38MAPK-positive cells resembling activated microglia were observed in the dorsal horn (Fig. 4C, Veh). Furthermore, the immunoreactivity was stronger and more extensive in p-p38MAPK-positive cells in the dorsal horn of vehicle or simulated AP-treated group as compared to minocycline and AP-treated groups (Fig. 4C). Densitometric analysis revealed that the fluorescent intensity in vehicle or simulated AP control was significantly higher than that in AP or minocycline group (Fig. 4C). To identify the cell types expressing p-p38MAPK, double labeling with Abs for p-p38MAPK and for cell-type specific markers (NeuN for Neurons, CC1 for oligodendrocytes, OX-42 for microglia, and GFAP for astrocytes) was performed. Results revealed that OX-42-positive microglia were positive for p-p38MAPK (Fig. 4D) whereas neurons, oligodendrocytes and astrocytes were negative for p-p38MAPK (data not shown). These data indicate that AP significantly attenuated p38MAPK activation in microglia after injury.

Analgesic effect by acupuncture is mediated through p38MAPK activation in microglia after SCI

To elucidate whether p38MAPK activation is involved in SCI-induced NP, SB203580, a p38MAPK inhibitor, was delivered

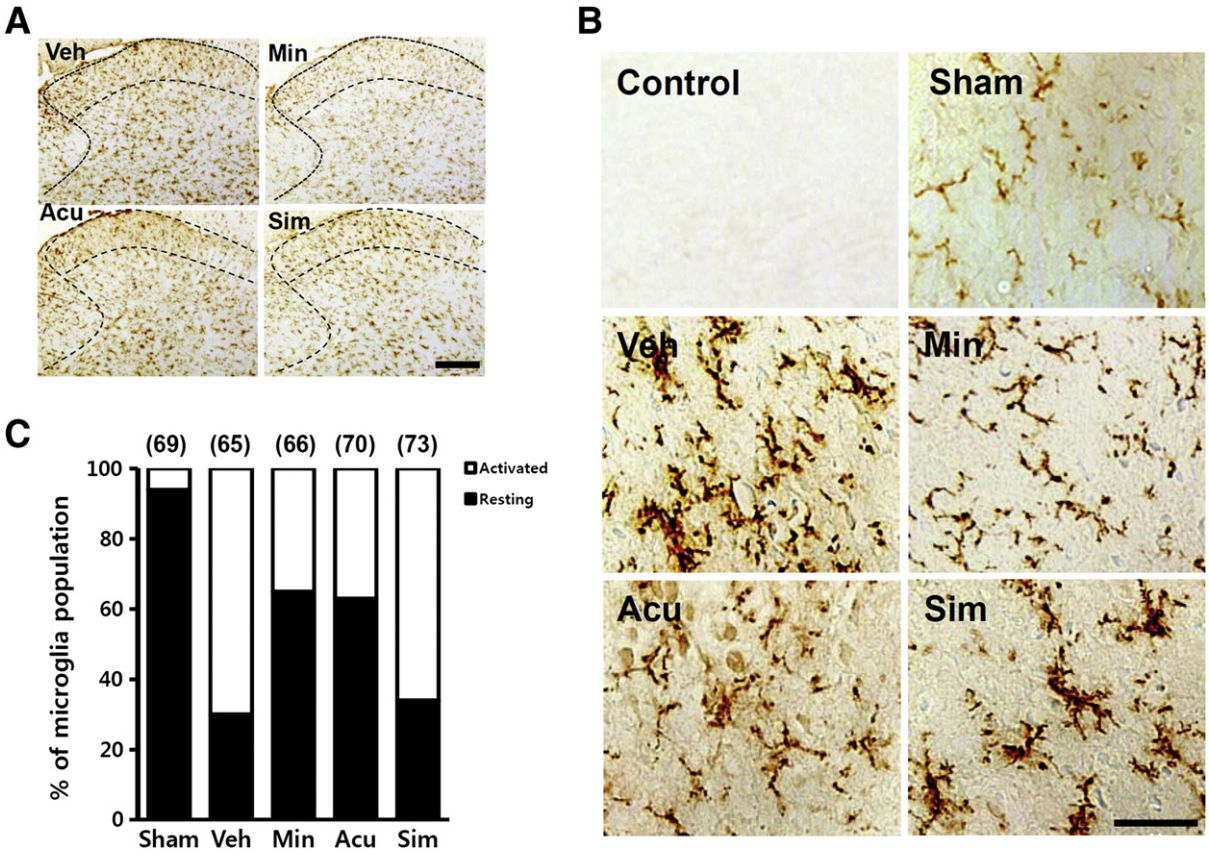

Fig. 3. Acupuncture inhibits microglial activation after SCI. At POD 33 after last treatment with AP, minocycline, simulated AP, and vehicle, lumbar (L4–5) spinal tissues were prepared and immunostained with microglial cell marker, OX-42 Ab (n = 5). (A) Low power views of OX-42-positive cells. Dotted line indicates lamina I and II in dorsal horn of the spinal cord. Scale bar, 100 μm. (B) High power views of OX-42 positive cells in lamina I and II. No positive signal was observed in the negative control in the absent of primary Ab (upper panel, Control). Scale bar, 30 μm. (C) Quantitative analyses show that AP or minocycline treatment significantly reduced the proportion of activated microglia when compared with that in the vehicle control. Resting and activated microglia were classified and counted as described in the Materials and methods section. Parentheses indicate the number of microglia sampled.

intrathecally via direct lumbar puncture on POD 31 once. AP and vehicle treatment were also done once. Administration of SB203580 (10 μg) alone showed significant increases in the mechanical PWT and thermal PWL at 2 h after post-injection as compared to vehicle control (SB203580 group: PWT; 7.4 ± 1.0 g and PWL; 9.0 ± 1.1 s vs. vehicle group: PWT; 1.0 ± 0.4 g and PWL; 5.0 ± 0.6 s; n = 6, $p<0.001$) (Figs. 5A, B). This result indicated that p38MAPK activation in microglia may mediate NP after SCI as reported (Hains and Waxman, 2006). Furthermore, the degree of the analgesic effects elicited by co-treatment of AP with SB203580 was significantly higher in both mechanical allodynia and thermal hyperalgesia at 2 h after post-injection when compared with SB203580 alone or AP alone (SB203580 + AP: PWT; 14.0 ± 0.4 g and PWL: 10.8 ± 1.5 s vs. AP alone: PWT; 7.5 ± 1.2 and PWL; 8.0 ± 0.8 s; n = 6, $p<0.05$) (Figs. 5A, B).

Acupuncture inhibits ERK activation after SCI

It was also known that ERK is activated in microglia in the spinal dorsal horn on delayed time and implicated in NP after SCI (Crown et al., 2006; Yu and Yezierski, 2005; Zhao et al., 2007). Therefore, we examined whether AP inhibits the activation of ERK after SCI and thereby alleviate SCI-induced NP. Western blotting using an Ab against p-ERK was performed on total extracts from L4–L5 lumbar spinal cord of rats treated with AP, minocycline, simulated AP and vehicle for 3 d. On POD 33, the level of p-ERK was increased as compared to sham control (data not shown) as reported (Crown et al., 2006; Yu and Yezierski, 2005). The level of p-ERK was significantly reduced in the AP-treated group when compared with vehicle control (AP group: 0.58 ± 0.04 vs. vehicle group: 1.0 ± 0.0; n = 4, $p<0.05$) (Figs. 6A, B). Minocycline treatment also resulted in a significant reduction in the level of p-ERK (minocycline group: 0.7 ± 0.05, n = 4, $p<0.05$) (Figs. 6A, B). However, simulated AP treatment did not change the level of p-ERK (simulated AP group: 0.98 ± 0.05, n = 4) (Figs. 6A, B). After SCI, the immunoreactivity of p-ERK was increased and mostly present in superficial lamina including lamina I–II of the L4–L5 spinal dorsal horn (Fig. 6C, Veh), while very low immunoreactivity of p-ERK was observed in sham control (Fig. 6C, Sham). The p-ERK immunoreactivity in lamina I and II was decreased in both AP- and minocycline-treated groups when compared with the vehicle or simulated AP-treated group (Fig. 6C). Densitometric analysis revealed that fluorescent intensity in AP- or minocycline-treated group was significantly lower than that in vehicle or simulated AP control (Fig. 6C). However, there was no marked difference in the fluorescent intensity in the deeper laminae III–IV or V–VI in all groups (data not shown). Furthermore, double labeling showed that p-ERK-positive cells were mostly expressed in microglia (Fig. 6D). Thus, these data indicate that AP inhibited ERK activation in microglia in the L4–L5 spinal dorsal horn after SCI.

To examine whether the analgesic effect of AP is also mediated by inhibiting ERK activation after SCI, PD98059, an ERK inhibitor, was delivered intrathecally into L4/5 spinal cord via direct lumbar puncture once on POD 31. AP and vehicle treatments were also done once. One hour after injection, PD98059 (10 μg) treatment alone exhibited significant increases in the mechanical PWT (PD98059

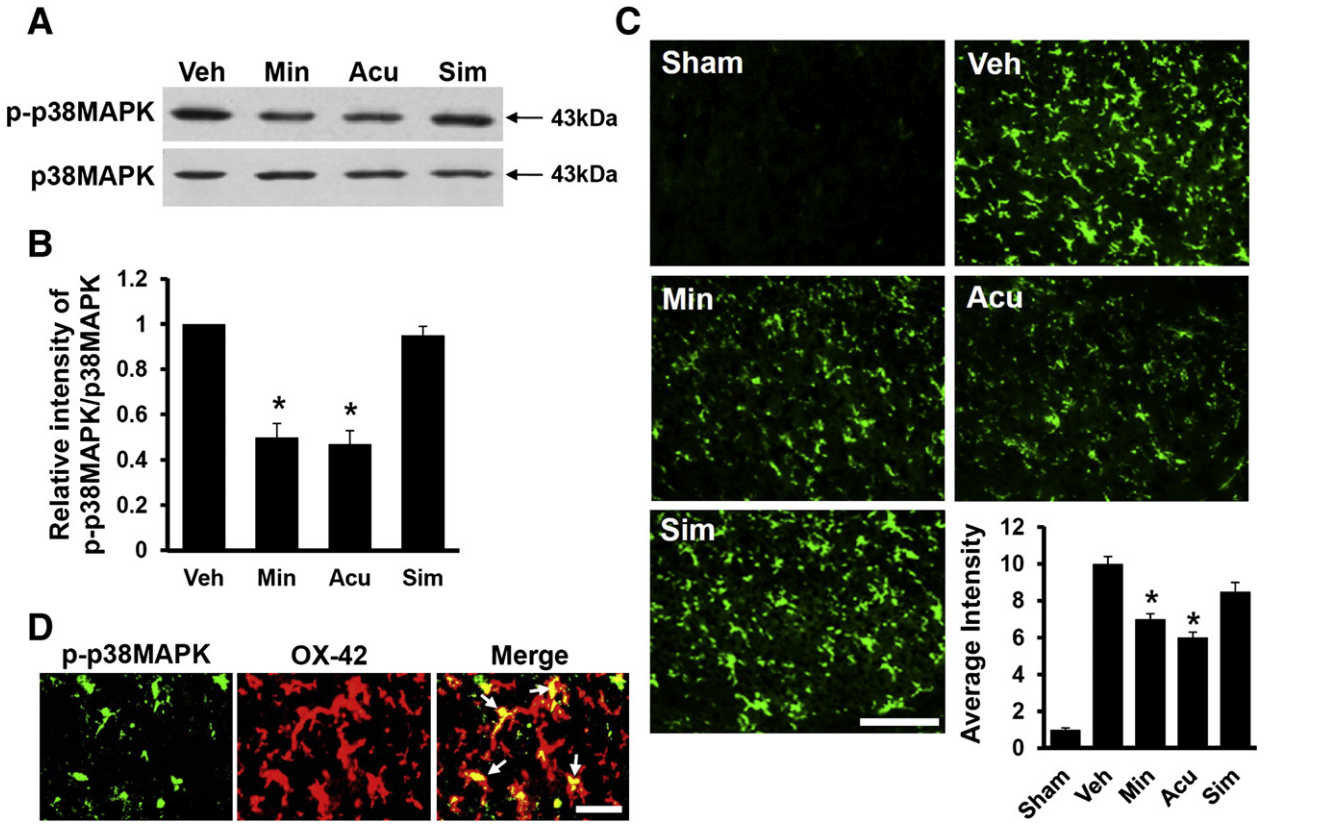

Fig. 4. Acupuncture inhibits p38MAPK activation after SCI. At POD 33 after last treatment with AP, minocycline, simulated AP, and vehicle, lumbar (L4–5) spinal tissues were isolated and total lysates were prepared (n = 4). (A) Western blot analysis of p-p38MAPK. (B) Quantitative analyses of Western blots show that AP or minocycline treatment significantly inhibited p38MAPK activation when compared with that in vehicle control. All data are presented as means ± SD of three separate experiments. $^{*}p<0.05$. (C) p-p38MAPK-positive cells in the spinal dorsal horn following SCI. Densitometric analysis reveals that AP or minocycline treatment significantly reduced the fluorescent intensity of p-p38MAPK as compared to that in vehicle control (n = 4). All data are presented as means ± SD of three separate experiments. $^{*}p<0.05$. (D) Double-labeled immunohistochemical analysis shows that OX-42-positive microglia expressed p-p38MAPK at 33 d after injury (arrows). Scale bars, 20 μm.

group: PWT; 6.3 ± 1.4 g vs. vehicle group: PWT; 1.0 ± 0.4 g; n = 6, $p<0.001$) and thermal PWL (PD98059 group: PWL; 7.8 ± 0.5 s vs. vehicle group: PWL; 5.1 ± 0.5 s; n = 6, $p<0.001$) as compared to the vehicle group (Figs. 7A, B). This result indicated that ERK activation in the dorsal horn at L4–L5 might mediate SCI-induced NP at below level. Furthermore, co-treatment of AP with PD98059 led to significant increases in mechanical PWT (PD98059 + AP: 10.5 ± 1.0 g vs. AP alone: 8.4 ± 1.5 g; n = 6, $p<0.05$) when compared with AP alone or PD98059 alone group (Figs. 7A, B).

Acupuncture inhibits ERK-dependent PGE2 production

PGE2 is produced in activated microglia in the lumbar spinal cord via ERK signaling and implicated in NP after SCI (Zhao et al., 2007). To

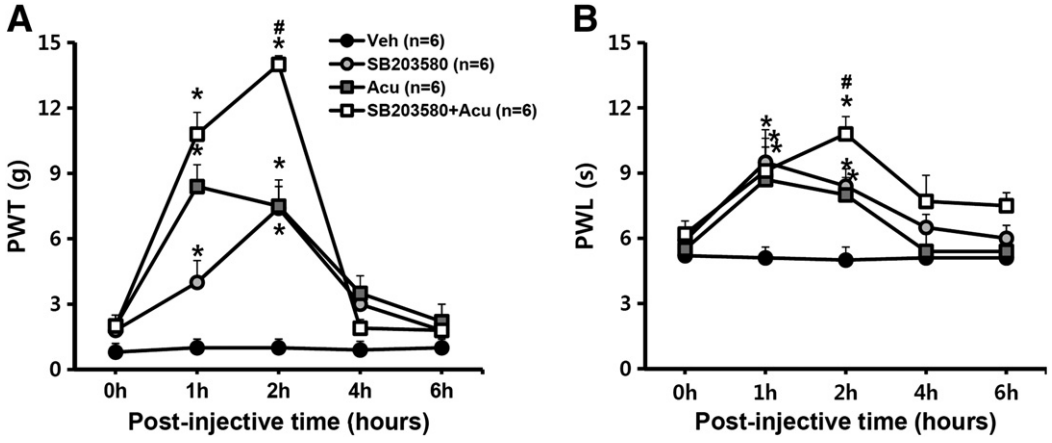

Fig. 5. Alleviation of neuropathic pain by acupuncture is mediated by inhibiting p38MAPK activation after SCI. SB203580 (10 μg/rat), an inhibitor of p38MAPK, was injected intrathecally (10 μl) once at POD 31 as described in the Materials and methods section (n = 6). (A and B) SB203580 treatment significantly increased mechanical PWT (A) and thermal PWL (B) when compared with those in vehicle control. Note that the degrees of the analgesic effects elicited by co-treatment of AP with SB203580 were significantly higher in both PWT and PWL than AP or SB203580 alone treated rats. All data are presented as means ± SD of three separate experiments. $^{*}p<0.001$ as compared to vehicle; $^{\#}p<0.05$ as compared to AP-treated rats.

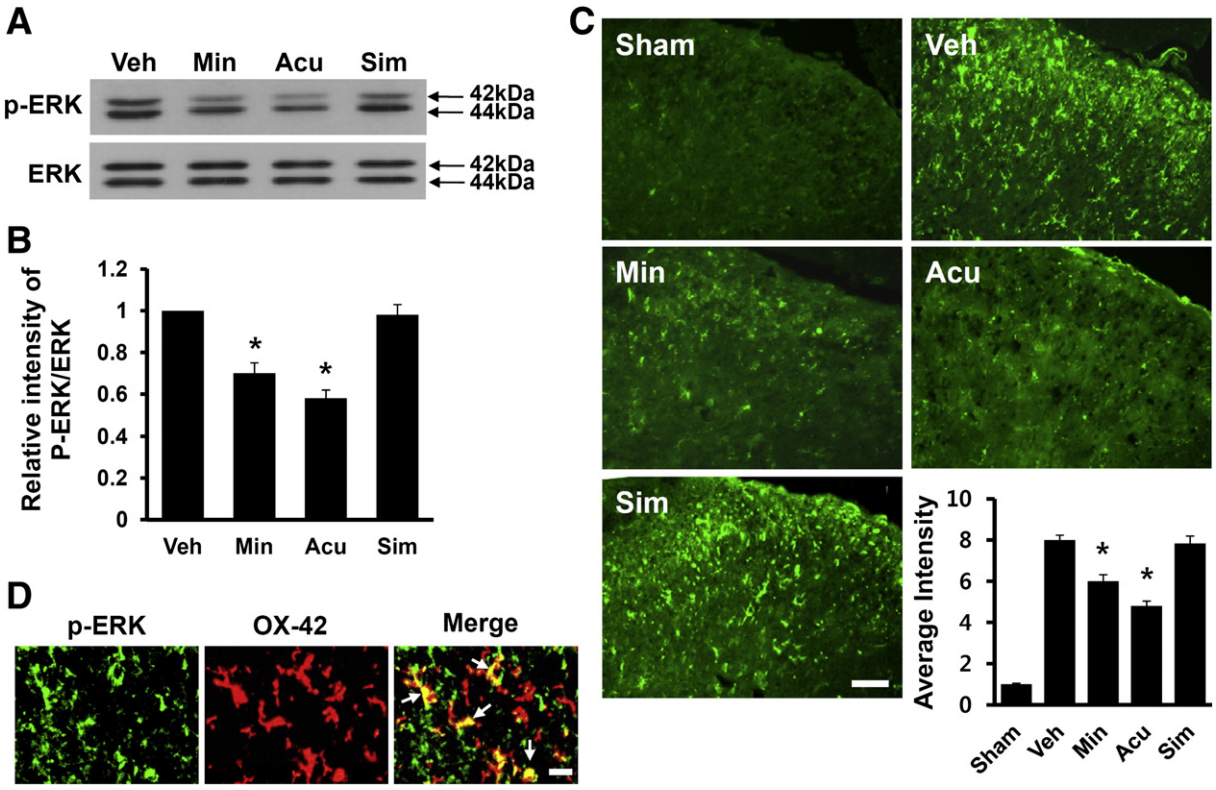

Fig. 6. Acupuncture reduces ERK activation after SCI. At POD 33 after last treatment with AP, minocycline, simulated AP, and vehicle, lumbar (L4–5) spinal tissues were isolated and total lysates were prepared (n = 4). (A) Western blots of p-ERK after injury. (B) Quantitative analysis of Western blots shows that AP or minocycline treatment significantly inhibited ERK activation when compared with that in vehicle control. All data are presented as means ± SD of three separate experiments. *$p<0.05$. (C) p-ERK-positive cells in the spinal dorsal horn (superficial layer) on POD 33 after SCI. Densitometric analysis reveals that AP or minocycline treatment significantly reduced the fluorescent intensity of p-ERK when compared with that in vehicle control (n = 4). Scale bar, 50 μm. All data are presented as means ± SD of three separate experiments. *$p<0.05$. (D) Double-labeled immunohistochemical analysis shows that OX-42-positive microglia expressed p-ERK at 33 d after injury (arrows). Scale bar, 20 μm.

determine whether AP suppresses the PGE2 production, enzyme immunoassay ELISA L4–L5 spinal extracts of animals treated once with sham, vehicle, minocycline, AP, PD98059 (ERK inhibitor) and AP + PD98059 on POD 31 was carried out. One hour after treatments, PGE2 levels in the L4–L5 lumbar spinal cords of vehicle group were significantly increased as compared to sham control (vehicle group: 740 ± 30 pg/ml vs. sham control; 365 ± 20 pg/ml; n = 5, $p<0.05$) (Fig. 8A). Administration of PD98059 or minocycline resulted in a significant reduction of the PGE2 levels when compared with vehicle (minocycline group: 500 ± 25 pg/ml, PD98059 group: 550 ± 25 pg/ml vs. vehicle group: 740 ± 30 pg/ml; n = 5, $p<0.05$) (Fig. 8A). This result indicates that PGE2 is produced via ERK signaling as reported (Zhao et al., 2007). Furthermore, the level of PGE2 was significantly reduced by AP treatment as compared to the vehicle (AP group: 450 ± 20 pg/ml, n = 5, $p<0.05$) (Fig. 8A). Especially, co-treatment of AP with PD98059 synergistically suppressed PGE production following SCI (AP + PD98059: 380 ± 26 pg/ml vs. AP alone: 450 ± 20 pg/ml, n = 5, $p<0.05$). These results further suggest that AP attenuates NP by decreasing ERK signaling-dependent PGE2 production in microglia after injury.

A recent report by Zhao et al. (2007) showed that PGE2 produced by ERK-dependent signaling mediates NP through PGE2 receptors (EP2) after SCI. Immunohistochemical study reveals that EP2 was

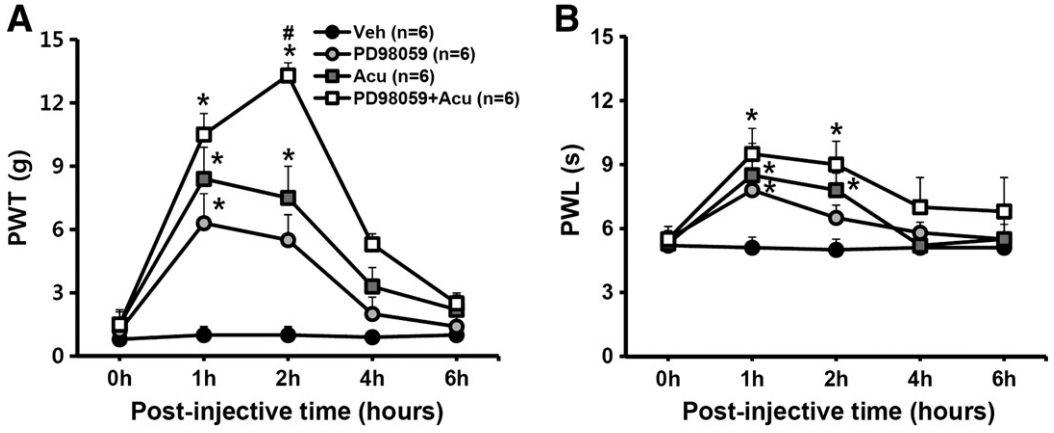

Fig. 7. Alleviation of neuropathic pain by acupuncture is mediated by inhibiting ERK activation after SCI. PD98059 (10 μg/rat, 10 μl), an inhibitor of ERK, was injected intrathecally once on POD 31 after injury as described in the Materials and methods section (n = 6). (A and B) PD98059 treatment significantly increased mechanical PWT (A) and thermal PWL (B) when compared with those in vehicle-treated rats. Note that the degree of the analgesic effect elicited by co-treatment of AP with PD98059 was significantly higher in PWT than AP or PD98059 alone treated rats. All data are presented as means ± SD of three separate experiments. *$p<0.001$ as compared to vehicle; #$p<0.05$ as compared to AP-treated rats.

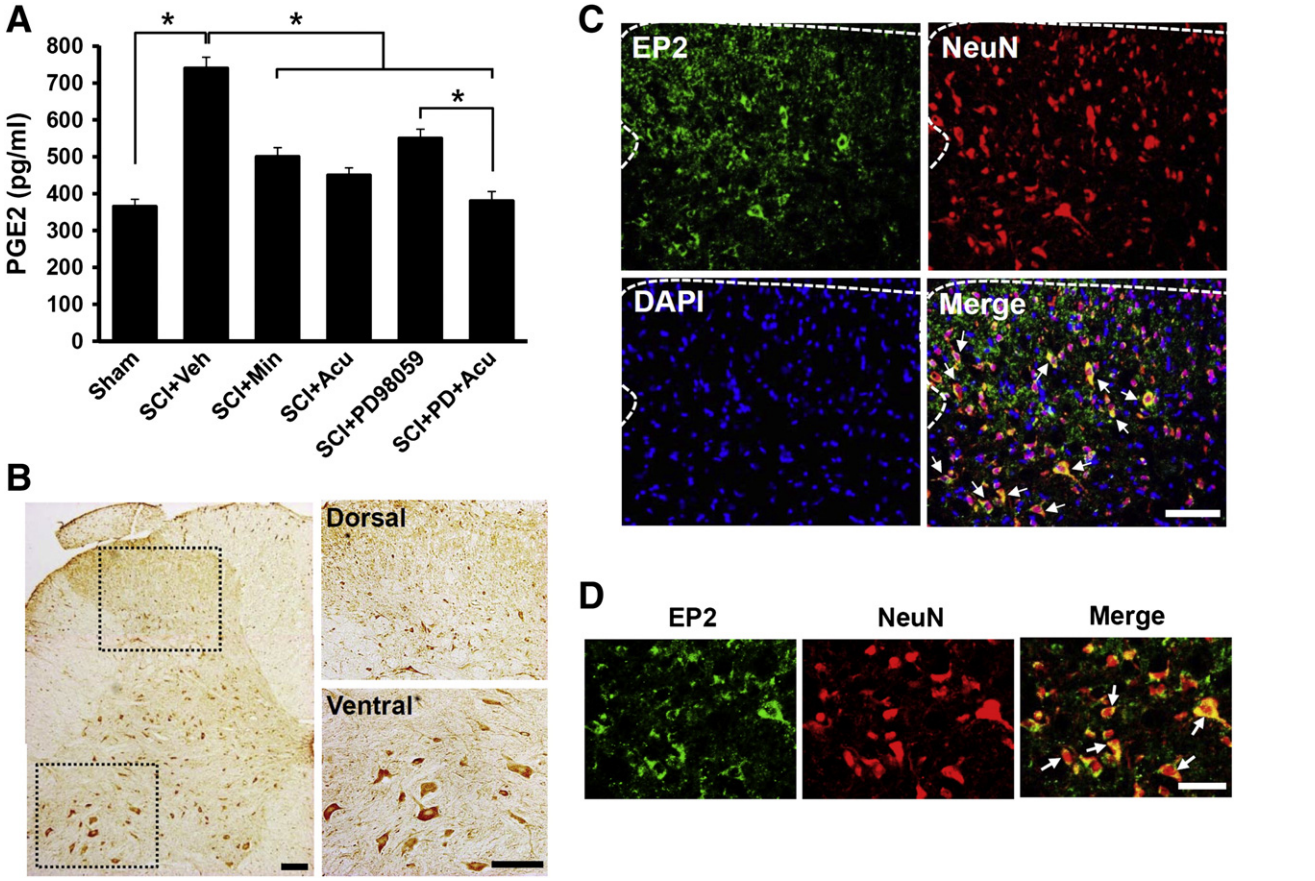

Fig. 8. Acupuncture reduces PGE2 level in the lumbar spinal cord after SCI. Injured rats were treated with AP, minocycline, PD98059, and AP + PD98059 at POD 31 and 1 h after treatment, lumbar (L4–5) spinal cord lysates were prepared and PGE2 levels were determined as described in the Method sections (n = 5). (A) PGE2 levels in the L4–L5 spinal cords. All data are presented as means ± SD of three separate experiments. *$p<0.05$. (B) Localization of EP2, PGE2 receptor, in the lumbar spinal cord. The right panels show higher power views of dorsal and ventral horn of the spinal cord shown in the left panel (rectangular areas). (C) Cellular localization of EP2 in the dorsal horn. EP2 signal was strong and confined to cells exhibiting morphological characteristics of neurons (NeuN-positive) in throughout of the spinal cord. (D) Double-labeled immunohistochemistry indicates that EP2 immunoreactivity was co-localized with NeuN-positive cells (arrows). Scale bars, 30 μm.

expressed in the gray matter (GM) including dorsal, intermediate and ventral horn of L4 spinal segment after injury (Fig. 8B). In sham control, EP2 immnuoreactivity was also observed (data not shown). Double labeling with Abs for cell type-specific markers showed that EP2 immunoreactivity was co-localized with NeuN, indicating EP2 is preferentially expressed in neurons (Figs. 8C, D), but not in microglia or astrocytes (data not shown).

AP inhibits superoxide anion production in microglia after SCI

A recent report shows that ROS produced in microglia in spinal nerve injury model for neuropathic pain play critical roles in activation and subsequent pain hypersensitivity (Kim et al., 2010). Therefore, we hypothesized that AP would inhibit ROS production in microglia and thereby relieve NP after SCI. First, we examined whether superoxide anion (O_2•), one of ROS, is produced in microglia and AP inhibits its production by using HEt, a fluorescent dye that is a specific indicator of O_2•. Fifteen min before AP or MnTBAP (a broad-spectrum ROS scavenger) treatment, 200 μl of HEt (1 mg/ml) was administered via intravenous injection. One hour after treatment, lumbar spinal tissues were prepared and sectioned as described above. As shown in Fig. 9A, strong Etd fluorescence was observed in laminae I and II as well as in the deeper layer of dorsal horn after SCI (Fig. 9A, Veh), whereas no fluorescence was observed in the sham-operated spinal cord (Fig. 9A, Sham). In addition, fluorescence intensity was stronger in the deeper layer than in laminae I and II. Since it has been known that superficial dorsal horn (laminae I and II) was related to receive nociception and pain signals from thinly myelinated and unmyelinated primary afferent fibers (Lu and Perl, 2005), we focused on the O_2• which produced in the superficial dorsal horn in the present study. On higher magnification, strong Etd fluorescence appeared as punctuated and dotted forms in the cytoplasm (Fig. 9A, Veh, bottom panel). Furthermore, in the AP-treated groups, the number of Etd-positive cells and Etd fluorescence intensity was markedly decreased as compared to vehicle or simulated AP control (Figs. 9A, B) (AP group: 10 ± 1.3 vs. vehicle group: 25 ± 2.2 or simulated AP group: 24 ± 2.4; n = 5, $p<0.05$). MnTBAP treatment via intrathecal injection also significantly reduced the intensity of Etd fluorescence as compared to vehicle or simulated AP groups (Figs. 9A, B) (MnTBAP: 8 ± 2.0; n = 5). Double-labeling with cell-type markers showed that most neurons in the deeper layer and microglia in the laminae I and II were positive for Etd, whereas astrocyte was negative for Etd (Fig. 9C).

Next, to determine the role of O_2• on SCI-induced NP, we examined the effect of MnTBAP on mechanical PWT and thermal PWL. As shown in Figs. 10A and B, MnTBAP treatment significantly increased in mechanical PWT (MnTBAP: 12.4 ± 0.9 g vs. Vehicle: 1.6 ± 0.5 g; n = 10, $p<0.001$) and thermal PWL (MnTBAP: 11.5 ± 0.8 s vs. Vehicle: 5.8 ± 0.5 s; n = 10, $p<0.001$) when compared with vehicle group (Figs. 10A, B). MnTBAP treatment also significantly inhibited the activation of p38MAPK and ERK as compared to vehicle group (p-p38MAPK, MnTBAP group: 1.2 ± 0.3 vs. vehicle group: 2.2 ± 0.3; p-ERK, MnTBAP group: 1.03 ± 0.4 g vs. vehicle group: 2.3 ± 0.2, n = 4, $p<0.05$) (Figs. 10C, D). Furthermore, MnTBAP treatment significantly decreased

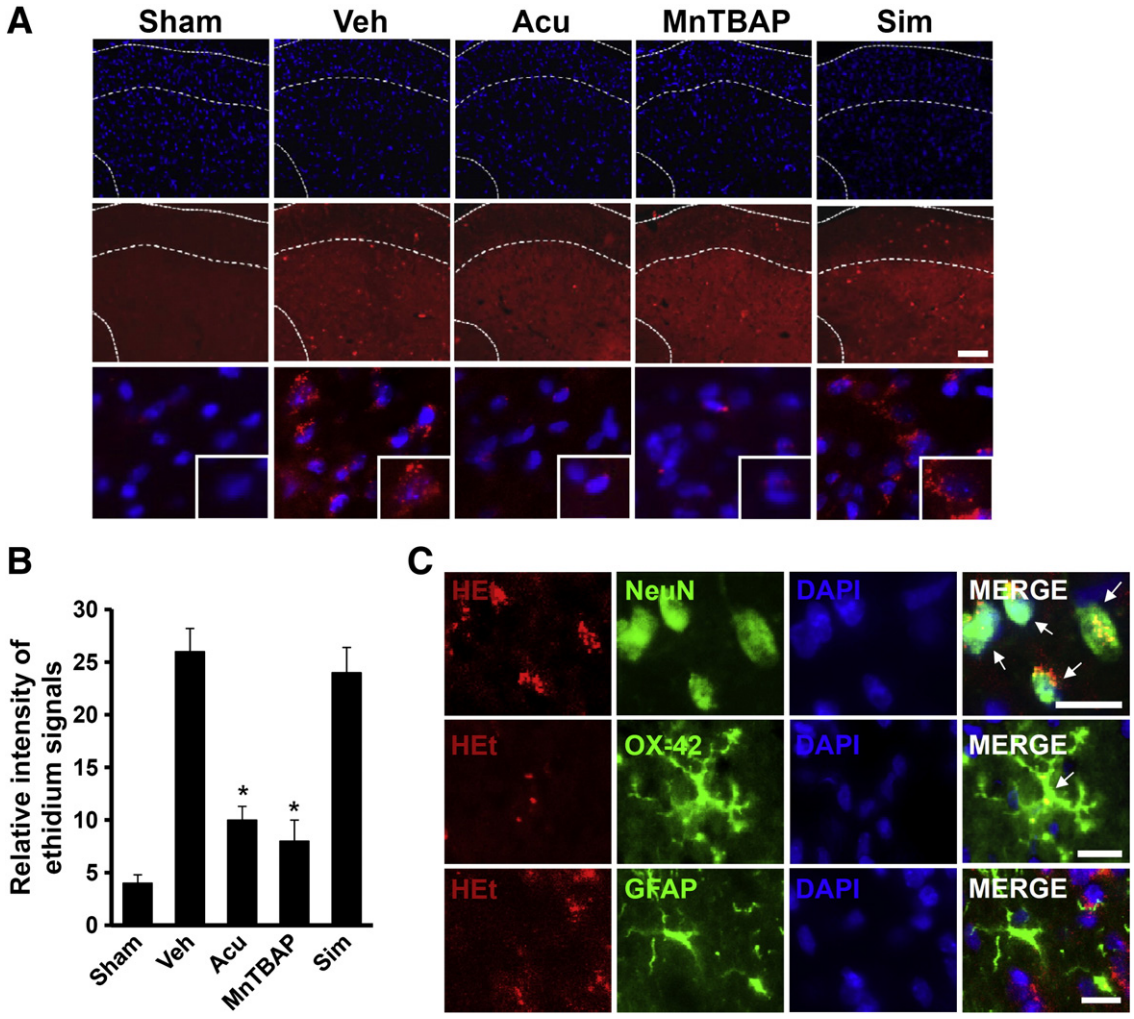

Fig. 9. Acupuncture inhibits superoxide anion production in dorsal horn of lumbar spinal cord after SCI. On POD 31, 15 min before AP or MnTBAP treatment, 200 μl of HEt (1 mg/ml) was injected intravenously as described in the Materials and methods section (n = 5). (A) Representative photographs of ethidium (Etd) fluorescence in spinal cord dorsal horn. The right, bottom panels show a higher magnification. Scale bar, 30 μm. (B) The relative Etd fluorescence intensity in the spinal dorsal horn (lamina I, II). Note that Etd fluorescence intensity was lower in AP or MnTBAP-treated groups than in the vehicle or simulated AP groups. Data represent the mean ± SD obtained from three experiments. *$p<0.05$. (C) Representative photographs of fluorescence microscopy show that neurons (NeuN) and microglia (OX-42) were HEt-positive (arrows) whereas astrocytes (GFAP) were not. Scale bars, 30 μm.

the proportion of activated microglia when compared with vehicle control group (MnTBAP group: 33.2 ± 0.77% vs. vehicle group: 72.1 ± 1.32%; n = 5, $p<0.05$) (data not shown). These results suggested that O_2• produced in microglia in the L4–L5 spinal dorsal horn induces p38MAPK and ERK activation, thereby mediates SCI-induced NP. Thus the analgesic effect of AP may be mediated by inhibiting ROS production in microglia.

Acupuncture also inhibits the expression of inflammatory mediators in the L4–L5 spinal dorsal horn after SCI

It is well documented that after SCI, activated microglia produce several inflammatory mediators such as IL-1β, IL-6, TNF-α, COX-2 and iNOS, which are known to mediate SCI-induced NP (Detloff et al., 2008; Hulsebosch, 2008; Yang et al., 2005b). Therefore, we examined the effect of AP treatment on the expression of inflammatory mediators by RT-PCR on POD 33 after 3 d treatments. The expression levels of IL-1β, IL-6, TNF-α, COX-2 and iNOS mRNA were significantly decreased by AP or minocycline while simulated AP had no significant effect on cytokine levels (n = 4, $p<0.05$) (Figs. 11A, B). ELISA assays also showed that AP treatment significantly inhibited the production of IL-1β, IL-6, and TNF-α after injury (AP group: IL-1β, IL-6 and TNF-α; 17 ± 4.0 pg/ml, 5 ± 4.1 pg/ml, 27 ± 3.2 pg/ml respectively vs. vehicle group: IL-1β, IL-6 and TNF-α; 55 ± 5.1 pg/ml, 30 ± 2.9 pg/ml, 80 ± 10.3 pg/ml respectively; n = 5, $p<0.05$) (Fig. 11C). By Western blot, the protein level of iNOS and COX-2 were also decreased by AP treatment as compared to vehicle or simulated AP groups (n = 5, $p<0.05$) (Figs. 11D, E).

Discussion

It has been reported that AP alleviates NP following peripheral nerve injury (Hwang et al., 2002; Lau et al., 2008; Park et al., 2010). However, the effects of AP on NP following CNS injuries such as SCI have not been reported, although several reports show that AP inhibits free radicals production and astrocyte proliferation, and increases the regeneration-related laminin expression and excitability of bladder smooth muscle after SCI (Wang et al., 2009; Wu et al., 2002; Yang et al., 2005a; Zhu, 2002). Our results show that AP treatment exerts a remarkable analgesic effect against SCI-induced NP at below level by inhibiting production of superoxide anion (O_2•) and microglial activation, thereby attenuating p38MAPK and ERK activation in microglia. These results are correlated with a recent our report showing that AP improves functional recovery by inhibiting apoptotic cell death via attenuation of microglial activation after SCI in rats (Choi et al., 2010). In the present study, in order to verify the effect of AP on microglial activation, minocycline, an inhibitor of inflammation,

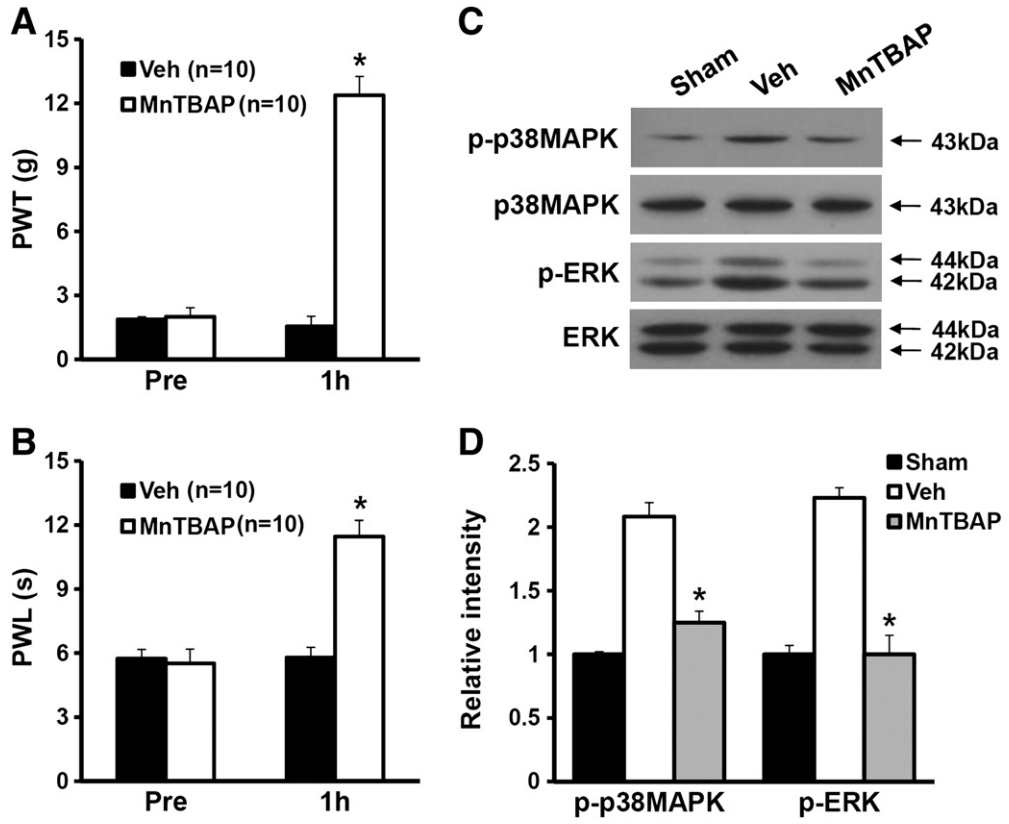

Fig. 10. Superoxide anion produced after injury induces p38MAPK and ERK activation and mediates SCI-induced neuropathic pain. MnTBAP (2.5 mg/kg) was injected intrathecally once at POD 31 and pain behavior test or spinal tissue was performed or prepared as described in the Materials and methods section. (A and B) MnTBAP treatment significantly increased mechanical PWT (A) and thermal PWL (B) when compared with that in vehicle-treated rats (n = 10). All data are presented as means ± SD of three separate experiments. *$p<0.001$. (C) Western blots of p-p38MAPK and p-ERK (n = 4). (D) Quantitative analysis of Western blots shows that MnTBAP treatment significantly decreased both p-p38MAPK and p-ERK levels when compared with those observed in vehicle control at 31 d after SCI. All data are presented as means ± SD of three separate experiments. *$p<0.05$.

was used as a positive control, which is known to inhibit SCI-induced below-level NP by inhibiting microglial activation (Hains and Waxman, 2006; Peng et al., 2006; Zhao et al., 2007). Together, our data indicate that SCI-induced NP is mediated by O_2• produced in microglia and the analgesic effects of AP are likely mediated in part by inhibiting O_2•-induced microglial activation after injury. Furthermore, to our knowledge, the present study is the first report showing the mechanistic role of AP's analgesic effect on SCI-induced NP.

Neuronal hyper-excitability plays a key role in central NP following SCI (Defrin et al., 2001; Finnerup et al., 2001). Although the cascade of acute pathophysiological events following SCI, which includes excitotoxicity, inflammation and cell death, results in progressive secondary degeneration, and this degeneration may contribute to the development of NP (Eide, 1998; Krenz and Weaver, 1998). However, the mechanisms underlying SCI-induced NP are not well understood. Here, our study provides an evidence for an association between microglial activation and chronic NP after SCI. Furthermore, as an answer the question how microglial activation can be inhibited by AP, we found that O_2• is produced in microglia as well as in neurons (see Fig. 9C) and microglial activation is significantly inhibited by treatment of MnTBAP, a ROS scavenger. These results are the first report showing the role of O_2• as a modulator on microglial activation in SCI-induced central NP and also correlates with the report by Kim et al. (2010) showing that NADPH oxidase 2-derived ROS produced in spinal cord microglia mediate peripheral nerve injury-induced NP. A recent study also showed that AP induces a release of adenosine as a neuromodulator, thereby mediates local anti-nociceptive effects of AP through adenosine A1 receptor (Goldman et al., 2010). ATP and a various purinergic receptors such as P2X4 and $P2Y_{12}$ expressed in activated microglia, are known to mediate NP signaling or neuronal hyper-excitability (Kobayashi et al., 2008; Tozaki-Saitoh et al., 2008; Tsuda et al., 2008; Ulmann et al., 2008). Thus, it would be interesting to find out whether AP inhibits production of some unknown modulators which trigger microglial activation after injury. In fact, our data showed that AP inhibits O_2• production, thereby microglial activation, which attenuate SCI-induced NP. Furthermore, our study demonstrated the possibility that O_2• produced in neurons located in dorsal horn could affect on neuronal hyper-excitability and AP may inhibit O_2•-induced neuronal hyper-excitability.

Recent study has been focused on the activation of key intracellular signaling cascades in the initiation and maintenance of central NP following SCI. In particular, p38MAPK and ERK MAPKs have been known to play roles in the maintenance of SCI-induced below-level pain (Crown et al., 2005, 2006; Hains and Waxman, 2006; Peng et al., 2006). The present study examined the effects of AP on these MAPKs activation and found their roles in SCI-induced NP by using pharmacological inhibitors. Our data showed that both p38MAPK and ERK are implicated in chronic NP after injury and the analgesic effects by AP are mediated in part by inhibiting p38MAPK and ERK activation. Also, we demonstrated that most p-p38MAPK and p-ERK up-regulation are localized in activated microglia within the lumbar dorsal horn after SCI (see Figs. 4, 6) as reported (Crown et al., 2008; Hains and Waxman, 2006). Furthermore, our data showed that O_2• produced in microglia induces p38MAPK and ERK activation and mediates SCI-induced mechanical allodynia and thermal hyperalgesia, which are inhibited by MnTBAP treatment. These results demonstrated that O_2• plays as an inducer for p38MAPK and ERK activation in SCI-induced NP.

PGE2 is known as a crucial mediator in the induction of central sensitization of spinal neurons as well as inflammatory pain sensitization (Bar et al., 2004; Harvey et al., 2004; Hosl et al., 2006). Also, ERK1/2 activation is known to be an upstream effector of the PGE2 production in microglia (Zhao et al., 2007). In the present study, at

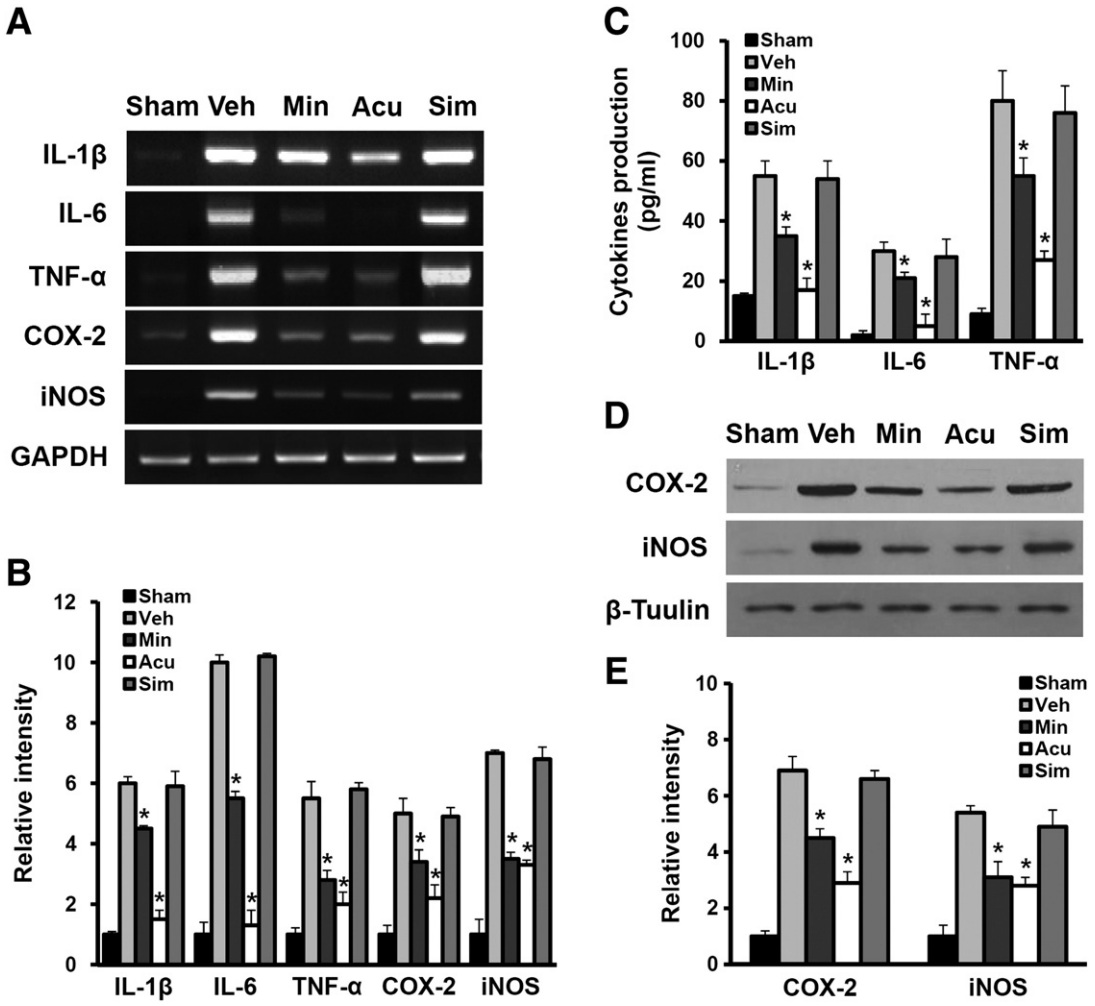

Fig. 11. Acupuncture inhibits the expression of inflammatory mediators in lumbar level of spinal cord after SCI. At 1 h after the last treatment with AP, minocycline, simulated AP, and vehicle at POD 33, total RNA from spinal cord samples were prepared as described in the Materials and methods section (n = 4). (A) RT-PCR of IL-1β, IL-6, TNF-α, COX-2 and iNOS mRNA. (B) Quantitative analysis of RT-PCR shows that AP or minocycline treatment significantly inhibited the expression of inflammatory mediators when compared with those in vehicle-treated rats at 33 d after injury. (C) ELISA of IL-1β, IL-6 and TNF-α (n = 5). (D) Western blots of COX-2 and iNOS (n = 5). (E) Quantitative analysis of Western blots. Note that AP also significantly inhibited the expression of COX-2 and iNOS. Data represent mean ± SD from three separate experiments. $^{*}p < 0.05$.

31 d after SCI, PGE2 levels in the lumbar spinal cord were significantly increased when compared with sham animals. Furthermore, an ERK inhibitor, PD98059, decreased PGE2 level and alleviated chronic NP, and AP significantly reduced PGE2 levels after injury, suggesting that the analgesic effects by AP may be mediated in part by inhibiting ERK-dependent PGE2 production after SCI. It has been known that PGE2, acting through the EP2 receptor located on dorsal horn neurons, directly depolarizes spinal neurons and thereby is sufficient to induce changes in their excitability state, which poises them to inappropriately amplify innocuous and noxious sensory stimuli (Baba et al., 2001; Zhao et al., 2007). Here, our data demonstrate that EP2 is localized on postsynaptic dorsal horn neurons as reported (Kawamura et al., 1997; Zhao et al., 2007) while the EP2 is not localized on microglia after SCI. Based on the study by Zhao et al. (2007), our study suggest that the analgesic effects by AP may be mediated by attenuating a putative microglia–neuron signaling mechanism mediated by ERK-dependent PGE2 released by activated microglia through EP2, which contributes to the sensitization of spinal neurons after SCI.

Activated microglia are known to actively participate in the generation of central sensitization by producing a various inflammatory mediators including IL-1β, IL-6, TNF-α, COX-2, and iNOS (Bingham et al., 2005; Gabay et al., 2011; Lee et al., 2010; Tanabe et al., 2009; Xu and Drew, 2006). For example, Lee et al. (2010) showed that IL-6 induces microglial CX3CR1 expression via p38MAPK activation, thereby contributes peripheral nerve injury-induced NP. Furthermore, intrathecal administration of anti-IL-6 Ab attenuates peripheral nerve injury-induced mechanical allodynia in the rat (Arruda et al., 2000). The report by Gustafson-Vickers et al. (2008) also shows that nerve-injury-induced release of IL-1β contributes to the central sensitization associated with chronic neuropathic pain. In addition, TNF-α produced after nerve injury induces long-term potentiation of C-fiber evoked field potentials in spinal dorsal horn in rats (Liu et al., 2007). Based on these reports, we predict that AP would also inhibit the expression of inflammatory mediators produced by activated microglia following SCI, thereby contributes in part to the analgesic effects of AP. In fact, our data show that AP decreases IL-1β, IL-6, TNF-α, iNOS, and COX-2 expression on POD 33 in L4–L5 lumbar spinal cord after injury.

In this study, we investigated that AP reduced SCI-induced NP in part by inhibiting O_2•-induced microglial activation after injury. However, it is still an open question on how a signal triggered by AP in the periphery reaches the CNS to modulate microglial activation. The effect of AP can result from the activation of particular population of primary afferents and modulation of descending control from the brainstem or release of a humoral factor. In addition, recent report shows that sensory neural activation of the soleus muscles activates

sympathetic neurons and increases CCL20 expression in dorsal blood vessels, thereby leads to entry of pathogenic CD4+ T cells at L5 cord in multiple sclerosis animal model (Arima et al., 2012). This report suggests that direct stimulation on peripheral nerves may affect body homeostasis. Based on this report, we suspect that the effect of AP can be mediated by regional neural activation, although we did not examine in this study.

Conclusively, we first demonstrated the therapeutic efficacy of AP in alleviation of chronic NP in an animal model of SCI. Our data show that AP significantly attenuates below-level pain following SCI by inhibiting microglial activation and inflammatory responses. Also, AP significantly inhibited $O_2^{\bullet}$-induced p38MAPK and ERK activation in microglia in the spinal dorsal horn of L4–L5 after injury. In addition, the production of PGE2 known to mediate SCI-induced NP was significantly attenuated by AP by inhibiting ERK signaling in microglia. Therefore, our data suggests that analgesic effects by AP may be mediated in part by inhibiting inflammatory responses via inhibition of MAPKs in activated microglia after SCI. Furthermore, drugs inhibiting ROS production in microglia and/or neuron may relieve chronic NP after SCI.

Acknowledgments

This study was supported by the Basic Science Research Program through the National Research Foundation of Korea (NRF) grant (No. 20110000932 (SRC)) and grants (2011K000291 and 2011K000282) from Brain Research Center of the 21st Century Frontier Research Program funded by the Ministry of Education, Science and Technology, the Republic of Korea.

References

Amit, Z., Galina, Z.H., 1986. Stress-induced analgesia: adaptive pain suppression. Physiol. Rev. 66, 1091–1120.
Arima, Y., Harada, M., Kamimura, D., Park, J.H., Kawano, F., Yull, F.E., Kawamoto, T., Iwakura, Y., Betz, U.A., Marquez, G., Blackwell, T.S., Ohira, Y., Hirano, T., Murakami, M., 2012. Regional neural activation defines a gateway for autoreactive T cells to cross the blood–brain barrier. Cell 148, 447–457.
Arruda, J.L., Sweitzer, S., Rutkowski, M.D., DeLeo, J.A., 2000. Intrathecal anti-IL-6 antibody and IgG attenuates peripheral nerve injury-induced mechanical allodynia in the rat: possible immune modulation in neuropathic pain. Brain Res. 879, 216–225.
Baastrup, C., Finnerup, N.B., 2008. Pharmacological management of neuropathic pain following spinal cord injury. CNS Drugs 22, 455–475.
Baba, H., Kohno, T., Moore, K.A., Woolf, C.J., 2001. Direct activation of rat spinal dorsal horn neurons by prostaglandin E2. J. Neurosci. 21, 1750–1756.
Bar, K.J., Natura, G., Telleria-Diaz, A., Teschner, P., Vogel, R., Vasquez, E., Schaible, H.G., Ebersberger, A., 2004. Changes in the effect of spinal prostaglandin E2 during inflammation: prostaglandin E (EP1–EP4) receptors in spinal nociceptive processing of input from the normal or inflamed knee joint. J. Neurosci. 24, 642–651.
Baron, R., 2006. Mechanisms of disease: neuropathic pain—a clinical perspective. Nat. Clin. Pract. Neurol. 2, 95–106.
Basso, D.M., Beattie, M.S., Bresnahan, J.C., 1995. A sensitive and reliable locomotor rating scale for open field testing in rats. J. Neurotrauma 12, 1–21.
Beric, A., 1997. Post-spinal cord injury pain states. Pain 72, 295–298.
Bernateck, M., Becker, M., Schwake, C., Hoy, L., Passie, T., Parlesak, A., Fischer, M.J., Fink, M., Karst, M., 2008. Adjuvant auricular electroacupuncture and autogenic training in rheumatoid arthritis: a randomized controlled trial. Auricular acupuncture and autogenic training in rheumatoid arthritis. Forsch. Komplementmed. 15, 187–193.
Bindokas, V.P., Jordan, J., Lee, C.C., Miller, R.J., 1996. Superoxide production in rat hippocampal neurons: selective imaging with hydroethidine. J. Neurosci. 16, 1324–1336.
Bingham, S., Beswick, P.J., Bountra, C., Brown, T., Campbell, I.B., Chessell, I.P., Clayton, N., Collins, S.D., Davey, P.T., Goodland, H., Gray, N., Haslam, C., Hatcher, J.P., Hunter, A.J., Lucas, F., Murkitt, G., Naylor, A., Pickup, E., Sargent, B., Summerfield, S.G., Stevens, A., Stratton, S.C., Wiseman, J., 2005. The cyclooxygenase-2 inhibitor GW406381X [2-(4-ethoxyphenyl)-3-[4-(methylsulfonyl)phenyl]-pyrazolo[1,5-b] pyridazine] is effective in animal models of neuropathic pain and central sensitization. J. Pharmacol. Exp. Ther. 312, 1161–1169.
Chaplan, S.R., Bach, F.W., Pogrel, J.W., Chung, J.M., Yaksh, T.L., 1994. Quantitative assessment of tactile allodynia in the rat paw. J. Neurosci. Methods 53, 55–63.
Cherkin, D.C., Sherman, K.J., Avins, A.L., Erro, J.H., Ichikawa, L., Barlow, W.E., Delaney, K., Hawkes, R., Hamilton, L., Pressman, A., Khalsa, P.S., Deyo, R.A., 2009. A randomized trial comparing acupuncture, simulated acupuncture, and usual care for chronic low back pain. Arch. Intern. Med. 169, 858–866.
Choi, D.C., Lee, J.Y., Moon, Y.J., Kim, S.W., Oh, T.H., Yune, T.Y., 2010. Acupuncture-mediated inhibition of inflammation facilitates significant functional recovery after spinal cord injury. Neurobiol. Dis. 39, 272–282.
Christensen, M.D., Hulsebosch, C.E., 1997. Chronic central pain after spinal cord injury. J. Neurotrauma 14, 517–537.
Christensen, M.D., Everhart, A.W., Pickelman, J.T., Hulsebosch, C.E., 1996. Mechanical and thermal allodynia in chronic central pain following spinal cord injury. Pain 68, 97–107.
Crown, E.D., Ye, Z., Johnson, K.M., Xu, G.Y., McAdoo, D.J., Westlund, K.N., Hulsebosch, C.E., 2005. Upregulation of the phosphorylated form of CREB in spinothalamic tract cells following spinal cord injury: relation to central neuropathic pain. Neurosci. Lett. 384, 139–144.
Crown, E.D., Ye, Z., Johnson, K.M., Xu, G.Y., McAdoo, D.J., Hulsebosch, C.E., 2006. Increases in the activated forms of ERK 1/2, p38 MAPK, and CREB are correlated with the expression of at-level mechanical allodynia following spinal cord injury. Exp. Neurol. 199, 397–407.
Crown, E.D., Gwak, Y.S., Ye, Z., Johnson, K.M., Hulsebosch, C.E., 2008. Activation of p38 MAP kinase is involved in central neuropathic pain following spinal cord injury. Exp. Neurol. 213, 257–267.
Defrin, R., Ohry, A., Blumen, N., Urca, G., 2001. Characterization of chronic pain and somatosensory function in spinal cord injury subjects. Pain 89, 253–263.
Detloff, M.R., Fisher, L.C., McGaughy, V., Longbrake, E.E., Popovich, P.G., Basso, D.M., 2008. Remote activation of microglia and pro-inflammatory cytokines predict the onset and severity of below-level neuropathic pain after spinal cord injury in rats. Exp. Neurol. 212, 337–347.
Eide, P.K., 1998. Pathophysiological mechanisms of central neuropathic pain after spinal cord injury. Spinal Cord 36, 601–612.
Finnerup, N.B., Johannesen, I.L., Sindrup, S.H., Bach, F.W., Jensen, T.S., 2001. Pain and dysesthesia in patients with spinal cord injury: a postal survey. Spinal Cord 39, 256–262.
Ford, G.K., Finn, D.P., 2008. Clinical correlates of stress-induced analgesia: evidence from pharmacological studies. Pain 140, 3–7.
Gabay, E., Wolf, G., Shavit, Y., Yirmiya, R., Tal, M., 2011. Chronic blockade of interleukin-1 (IL-1) prevents and attenuates neuropathic pain behavior and spontaneous ectopic neuronal activity following nerve injury. Eur. J. Pain 15, 242–248.
Goldman, N., Chen, M., Fujita, T., Xu, Q., Peng, W., Liu, W., Jensen, T.K., Pei, Y., Wang, F., Han, X., Chen, J.F., Schnermann, J., Takano, T., Bekar, L., Tieu, K., Nedergaard, M., 2010. Adenosine A1 receptors mediate local anti-nociceptive effects of acupuncture. Nat. Neurosci. 13, 883–888.
Gustafson-Vickers, S.L., Lu, V.B., Lai, A.Y., Todd, K.G., Ballanyi, K., Smith, P.A., 2008. Long-term actions of interleukin-1beta on delay and tonic firing neurons in rat superficial dorsal horn and their relevance to central sensitization. Mol. Pain 4, 63.
Hains, B.C., Waxman, S.G., 2006. Activated microglia contribute to the maintenance of chronic pain after spinal cord injury. J. Neurosci. 26, 4308–4317.
Hains, B.C., Yucra, J.A., Hulsebosch, C.E., 2001. Reduction of pathological and behavioral deficits following spinal cord contusion injury with the selective cyclooxygenase-2 inhibitor NS-398. J. Neurotrauma 18, 409–423.
Hargreaves, K., Dubner, R., Brown, F., Flores, C., Joris, J., 1988. A new and sensitive method for measuring thermal nociception in cutaneous hyperalgesia. Pain 32, 77–88.
Harvey, R.J., Depner, U.B., Wassle, H., Ahmadi, S., Heindl, C., Reinold, H., Smart, T.G., Harvey, K., Schutz, B., bo-Salem, O.M., Zimmer, A., Poisbeau, P., Welzl, H., Wolfer, D.P., Betz, H., Zeilhofer, H.U., Muller, U., 2004. GlyR alpha3: an essential target for spinal PGE2-mediated inflammatory pain sensitization. Science 304, 884–887.
Hosl, K., Reinold, H., Harvey, R.J., Muller, U., Narumiya, S., Zeilhofer, H.U., 2006. Spinal prostaglandin E receptors of the EP2 subtype and the glycine receptor alpha3 subunit, which mediate central inflammatory hyperalgesia, do not contribute to pain after peripheral nerve injury or formalin injection. Pain 126, 46–53.
Hulsebosch, C.E., 2008. Gliopathy ensures persistent inflammation and chronic pain after spinal cord injury. Exp. Neurol. 214, 6–9.
Hwang, B.G., Min, B.I., Kim, J.H., Na, H.S., Park, D.S., 2002. Effects of electroacupuncture on the mechanical allodynia in the rat model of neuropathic pain. Neurosci. Lett. 320, 49–52.
Hylden, J.L., Wilcox, G.L., 1980. Intrathecal morphine in mice: a new technique. Eur. J. Pharmacol. 67, 313–316.
Kang, J.M., Park, H.J., Choi, Y.G., Choe, I.H., Park, J.H., Kim, Y.S., Lim, S., 2007. Acupuncture inhibits microglial activation and inflammatory events in the MPTP-induced mouse model. Brain Res. 1131, 211–219.
Kawamura, T., Akira, T., Watanabe, M., Kagitani, Y., 1997. Prostaglandin E1 prevents apoptotic cell death in superficial dorsal horn of rat spinal cord. Neuropharmacology 36, 1023–1030.
Kim, D., You, B., Jo, E.K., Han, S.K., Simon, M.I., Lee, S.J., 2010. NADPH oxidase 2-derived reactive oxygen species in spinal cord microglia contribute to peripheral nerve injury-induced neuropathic pain. Proc. Natl. Acad. Sci. U. S. A. 107, 14851–14856.
Kobayashi, K., Yamanaka, H., Fukuoka, T., Dai, Y., Obata, K., Noguchi, K., 2008. P2Y12 receptor upregulation in activated microglia is a gateway of p38 signaling and neuropathic pain. J. Neurosci. 28, 2892–2902.
Krenz, N.R., Weaver, L.C., 1998. Effect of spinal cord transection on N-methyl-D-aspartate receptors in the cord. J. Neurotrauma 15, 1027–1036.
Lau, W.K., Chan, W.K., Zhang, J.L., Yung, K.K., Zhang, H.Q., 2008. Electroacupuncture inhibits cyclooxygenase-2 up-regulation in rat spinal cord after spinal nerve ligation. Neuroscience 155, 463–468.
Lee, S., Zhao, Y.Q., Ribeiro-da-Silva, A., Zhang, J., 2010. Distinctive response of CNS glial cells in oro-facial pain associated with injury, infection and inflammation. Mol. Pain 6, 79.
Levendoglu, F., Ogun, C.O., Ozerbil, O., Ogun, T.C., Ugurlu, H., 2004. Gabapentin is a first line drug for the treatment of neuropathic pain in spinal cord injury. Spine (Phila Pa 1976) 29, 743–751.
Liu, J., Feng, X., Yu, M., Xie, W., Zhao, X., Li, W., Guan, R., Xu, J., 2007. Pentoxifylline attenuates the development of hyperalgesia in a rat model of neuropathic pain. Neurosci. Lett. 412, 268–272.

Lu, Y., Perl, E.R., 2005. Modular organization of excitatory circuits between neurons of the spinal superficial dorsal horn (laminae I and II). J. Neurosci. 25, 3900–3907.
Mestre, C., Pelissier, T., Fialip, J., Wilcox, G., Eschalier, A., 1994. A method to perform direct transcutaneous intrathecal injection in rats. J. Pharmacol. Toxicol. Methods 32, 197–200.
Parisod, E., Siddall, P.J., Viney, M., McClelland, J.M., Cousins, M.J., 2003. Allodynia after acute intrathecal morphine administration in a patient with neuropathic pain after spinal cord injury. Anesth. Analg. 97, 183–186.
Park, J.H., Han, J.B., Kim, S.K., Park, J.H., Go, D.H., Sun, B., Min, B.I., 2010. Spinal GABA receptors mediate the suppressive effect of electroacupuncture on cold allodynia in rats. Brain Res. 1322, 24–29.
Peng, X.M., Zhou, Z.G., Glorioso, J.C., Fink, D.J., Mata, M., 2006. Tumor necrosis factor-alpha contributes to below-level neuropathic pain after spinal cord injury. Ann. Neurol. 59, 843–851.
Siddall, P.J., Taylor, D.A., Cousins, M.J., 1997. Classification of pain following spinal cord injury. Spinal Cord 35, 69–75.
Tan, A.M., Zhao, P., Waxman, S.G., Hains, B.C., 2009. Early microglial inhibition preemptively mitigates chronic pain development after experimental spinal cord injury. J. Rehabil. Res. Dev. 46, 123–133.
Tanabe, S.I., Bodet, C., Grenier, D., 2009. Treponema denticola peptidoglycan induces the production of inflammatory mediators and matrix metalloproteinase 9 in macrophage-like cells. J. Periodontal Res. 44, 503–510.
To, T.P., Lim, T.C., Hill, S.T., Frauman, A.G., Cooper, N., Kirsa, S.W., Brown, D.J., 2002. Gabapentin for neuropathic pain following spinal cord injury. Spinal Cord 40, 282–285.
Tozaki-Saitoh, H., Tsuda, M., Miyata, H., Ueda, K., Kohsaka, S., Inoue, K., 2008. P2Y12 receptors in spinal microglia are required for neuropathic pain after peripheral nerve injury. J. Neurosci. 28, 4949–4956.
Tsuda, M., Toyomitsu, E., Komatsu, T., Masuda, T., Kunifusa, E., Nasu-Tada, K., Koizumi, S., Yamamoto, K., Ando, J., Inoue, K., 2008. Fibronectin/integrin system is involved in P2X(4) receptor upregulation in the spinal cord and neuropathic pain after nerve injury. Glia 56, 579–585.
Ulmann, L., Hatcher, J.P., Hughes, J.P., Chaumont, S., Green, P.J., Conquet, F., Buell, G.N., Reeve, A.J., Chessell, I.P., Rassendren, F., 2008. Up-regulation of P2X4 receptors in spinal microglia after peripheral nerve injury mediates BDNF release and neuropathic pain. J. Neurosci. 28, 11263–11268.
Wang, J., Kawamata, M., Namiki, A., 2005. Changes in properties of spinal dorsal horn neurons and their sensitivity to morphine after spinal cord injury in the rat. Anesthesiology 102, 152–164.
Wang, J.H., Chen, B.G., Yin, J., Wang, G., Zou, W.G., Luo, X.J., 2009. Effect of electroacupuncture of different acupoints on the excitability of detrusor muscle and the expression of BDNF and TrkB in the spinal cord of rats with urinary retention due to spinal cord injury. Zhen Ci Yan Jiu 34, 387–392.
Woolf, C.J., Mannion, R.J., 1999. Neuropathic pain: aetiology, symptoms, mechanisms, and management. Lancet 353, 1959–1964.
Wu, Y., Sun, Z., Li, Z., Zhao, Y., Sun, S., 2002. Effect of acupuncture on free radicals in rats with early experimental spinal cord injury. J. Tradit. Chin. Med. 22, 51–54.
Xu, J., Drew, P.D., 2006. 9-Cis-retinoic acid suppresses inflammatory responses of microglia and astrocytes. J. Neuroimmunol. 171, 135–144.
Yang, C., Li, B., Liu, T.S., Zhao, D.M., Hu, F.A., 2005a. Effect of electroacupuncture on proliferation of astrocytes after spinal cord injury. Zhongguo Zhen Jiu 25, 569–572.
Yang, L., Jones, N.R., Blumbergs, P.C., Van Den, H.C., Moore, E.J., Manavis, J., Sarvestani, G.T., Ghabriel, M.N., 2005b. Severity-dependent expression of pro-inflammatory cytokines in traumatic spinal cord injury in the rat. J. Clin. Neurosci. 12, 276–284.
Yin, C.S., Jeong, H.S., Park, H.J., Baik, Y., Yoon, M.H., Choi, C.B., Koh, H.G., 2008. A proposed transpositional acupoint system in a mouse and rat model. Res. Vet. Sci. 84, 159–165.
Yu, C.G., Yezierski, R.P., 2005. Activation of the ERK1/2 signaling cascade by excitotoxic spinal cord injury. Brain Res. Mol. Brain Res. 138, 244–255.
Yune, T.Y., Lee, J.Y., Jung, G.Y., Kim, S.J., Jiang, M.H., Kim, Y.C., Oh, Y.J., Markelonis, G.J., Oh, T.H., 2007. Minocycline alleviates death of oligodendrocytes by inhibiting pro-nerve growth factor production in microglia after spinal cord injury. J. Neurosci. 27, 7751–7761.
Yune, T.Y., Lee, J.Y., Jiang, M.H., Kim, D.W., Choi, S.Y., Oh, T.H., 2008. Systemic administration of PEP-1-SOD1 fusion protein improves functional recovery by inhibition of neuronal cell death after spinal cord injury. Free Radic. Biol. Med. 45, 1190–1200.
Zhang, H., Cang, C.L., Kawasaki, Y., Liang, L.L., Zhang, Y.Q., Ji, R.R., Zhao, Z.Q., 2007. Neurokinin-1 receptor enhances TRPV1 activity in primary sensory neurons via PKCepsilon: a novel pathway for heat hyperalgesia. J. Neurosci. 27, 12067–12077.
Zhao, P., Waxman, S.G., Hains, B.C., 2007. Extracellular signal-regulated kinase-regulated microglia-neuron signaling by prostaglandin E2 contributes to pain after spinal cord injury. J. Neurosci. 27, 2357–2368.
Zhu, Z., 2002. Effects of electroacupuncture on laminin expression after spinal cord injury in rats. Zhongguo Zhong Xi Yi Jie He Za Zhi 22, 525–527.